A structural concept for a demountable glass column

An explorative design study about interlocking, laminated glass components

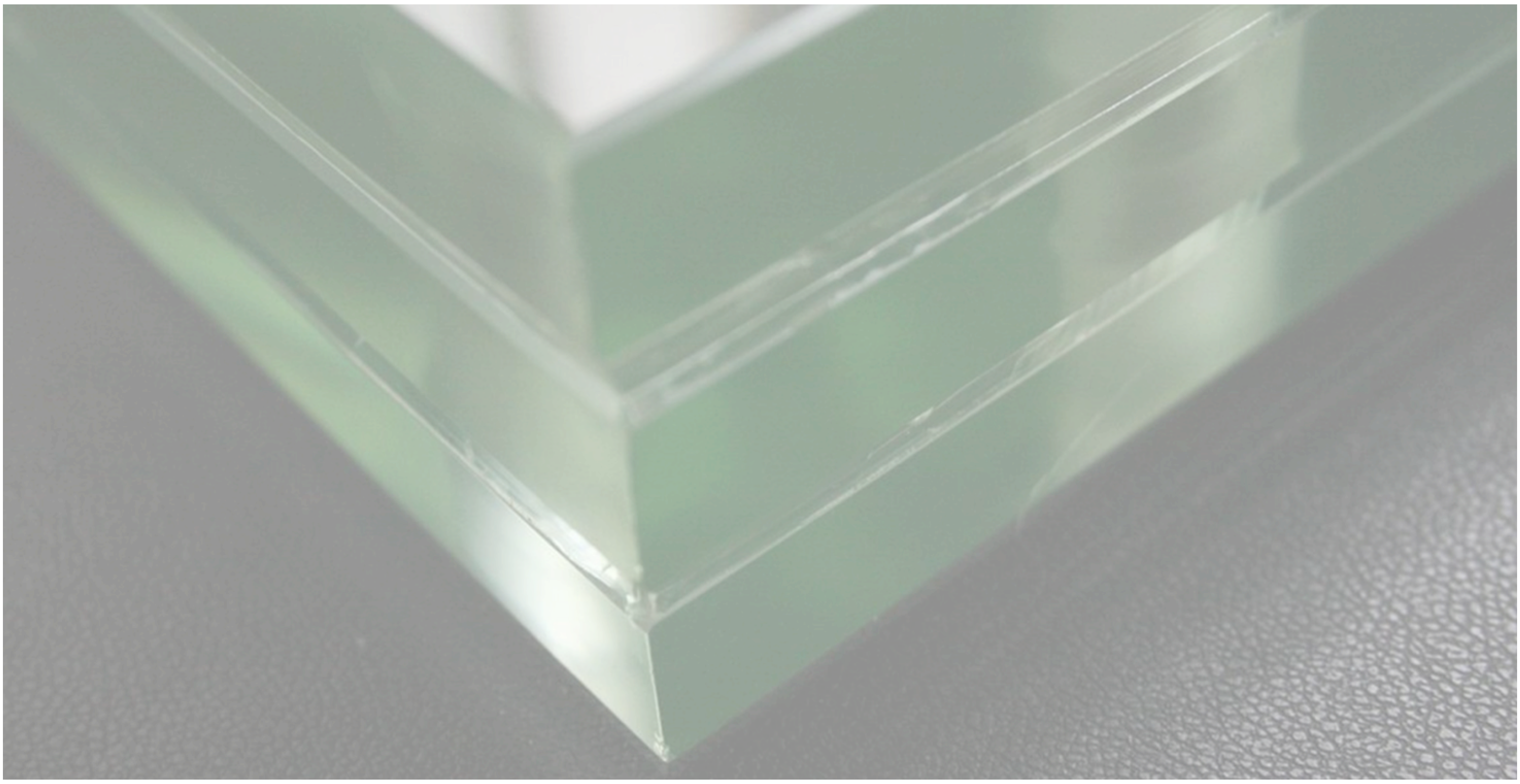

T.C. Verduyn

TU Delft

A structural concept for a demountable glass column

An explorative design study about interlocking, laminated glass components

by

T.C. Verduyn

Graduation committee:

Prof.ir. Rob Nijsse
Dr.ir. Max Hendriks
ir. Telesilla Bristogianni
ir. Faidra Oikonomopoulou

TU Delft

Preface

Before you lies my graduation thesis to complete the MSc Building Engineering of the faculty Civil Engineering at the TU Delft. This thesis is about the feasibility of a completely new type of glass column, made up of interlocking, laminated glass components. This topic fits perfectly with my interest in both architecture and civil engineering. For this research both aesthetics and a broader investigation of different structural parameters were important. I learned a lot during my graduation; Finite Element Analysis and Diana were completely new to me before starting.

First of all, I would like to thank my graduation committee for their guidance during this process. Firstly, Rob for his practical problem solving approach; Telesilla and Faidra for their strong conceptual thinking and enthusiasm for glass and Max for his extensive knowledge, guidance and help using Diana. Most of all, I would like to thank my mother and aunt for always being proud of me and for supporting my decisions all throughout my studies. Furthermore, I would like to thank my friends and study buddies for their companionship. Last but not least, a big thanks to Arjan for his patience, understanding and support during my graduation and in general.

T.C. Verduyn
Delft, August 22, 2018

Abstract

The high compressive strength of the material glass in combination with its transparency, make it an attractive material to use for a column. Though different types and configurations of glass columns have been subject of academic research, a demountable glass column made from laminated components remains unexplored. This structural concept allows for modular and temporary structures with incorporated structural safety. Assembly and demounting is quick and the smaller, laminated components give the column sufficient redundancy.

Glass however, is notorious for its low tensile strength and brittle failure. Also, a column made from interlocking components introduces stability problems. A comprehensive understanding of this new type of glass column is necessary before application in the built environment is possible. So far, no numerical analysis has been conducted on columns made up of interlocking laminated elements, while this analysis can help understand the stability, force distribution and stress concentrations of such a system.

The main objective of this research is to obtain a feasible all-glass column design. This is achieved by using a Finite Element Analysis (FEA) to investigate: stability, force distribution and stress concentrations. Furthermore, a variety of design aspects and trade-offs are discussed in detail. These structural and design considerations are used to iterate the column design and to propose a combination of parameters that leads to a feasible design.

The FEA investigates the following structural parameters: component dimension, roof ballast load, façade stiffness and interlayer thickness. Different combinations of investigated parameters lead to a feasible, functioning column designs. The column is able to horizontally displace up to 9,1 mm before becoming unstable. The heavier ballast load of 1,2 kN/m^2 is desired over the minimal value of 0,6 kN/m^2. The column is unable to take up a significant amount of the total horizontal case study load for all investigated component widths. It can take up up to 39 % of the vertically applied load when a minimal amount of soft interlayers is used. The tensile stress concentrations stay within the allowable limits.

The different design aspects investigated include: material constraints, fabrication limitations, safety and redundancy and assembly. Each laminated component is made of up 3 x 15 mm thick annealed float glass plates, and is fit with a sacrificial layer on either side for protection. The glass plates are water jet cut into the desired shape and then laminated together to form the component. The shape of the interlock is gradual end rounded in order to prevent (tensile) peak stresses. The risk of damage has been minimised. Moreover, the glass column has sufficient redundancy because the laminated components retain sufficient bearing capacity in case of damage. Also, the structural glass façade serves as secondary loading path in the case of severe damage.

This research serves as a starting point for future research and possible real-life application of a novel type of interlocking glass column. This type of column can be applied in demountable structures. Combinations of parameters have been proposed that result in a feasible, functioning column. Recommendations have been set up to improve future iterations of columns with a similar design.

Contents

I Introduction

1 Introduction 3
1.1 Problem statement 3
1.2 Research objectives 5
1.3 Methodology 5
1.4 Report outline 7

II Theoretical Framework

2 Glass structures 11
2.1 Introduction 11
2.2 Glass columns 11
2.2.1 Profiled glass column 12
2.2.2 Layered tubular column 13
2.2.3 Stacked column 13
2.2.4 Bundled column 14
2.2.5 Cast column 15
2.2.6 End connections 15
2.2.7 Comparison glass columns 16
2.3 Glass building envelopes 17
2.3.1 Building envelopes with metal substructure 17
2.3.2 Building envelopes with adhesively bonded elements 18
2.3.3 Building envelopes using interlocking geometry 18

3 Glass: the material . . . 19
3.1 Introduction 19
3.2 Production process 19
3.3 Post processing 20
3.4 Heat treatment 21
3.5 Lamination 21
3.6 Material properties 22
3.6.1 Brittle failure . . . 22
3.6.2 Flaws . . . 22
3.6.3 Strength . . . 23
3.7 Safety and design 23
3.7.1 Risks . . . 24
3.7.2 Risk reduction . . . 24
3.7.3 Fire safety for glass . . . 24
3.8 Recycling and sustainability 25
4 Demountable glass construction . . . 27
4.1 Introduction 27
4.2 Interlocking mechanisms glass 27
4.3 Dry interlayers 29
4.4 Boundary conditions interlocking structures 30
4.5 Conclusions demountable glass construction 30
III Analytical & Numerical Analysis
5 Analytical predictions . . . 33
5.1 Introduction 33
5.2 Column buckling 33
5.2.1 Buckling due to eccentric loading . . . 34
5.2.2 Buckling due to initial out-of-straightness . . . 35
5.2.3 Conclusions buckling . . . 36
5.3 Bending moment capacity column 36
5.4 Force distribution 37
6 Model description . . . 39
6.1 Introduction 39
6.2 Finite Element Model input 39
6.2.1 Geometry set up . . . 39
6.2.2 Loading conditions . . . 41
6.2.3 Model input properties . . . 41
6.3 Parameter investigation 43
6.4 Validity of model 43
6.4.1 Interface elements . . . 44
6.4.2 Displacements . . . 45

6.4.3 Reaction forces . . . 45

7 FEM Results . . . 47
7.1 Introduction 47
7.2 Stability 48
7.3 Force distribution 50
7.3.1 Horizontal force distribution . . . 50
7.3.2 Vertical force distribution . . . 51
7.4 Stress distribution 52
7.5 Outcome parameter study 53

IV Case Study

8 Design considerations . . . 57
8.1 Introduction case study 57
8.2 Conceptual design 57
8.3 Loading conditions 58
8.4 Design choices & motivations 58
8.4.1 Material choice . . . 58
8.4.2 Load transfer column . . . 58
8.4.3 Load transfer pavilion . . . 60
8.4.4 Element design . . . 61
8.4.5 Top & bottom connections . . . 62
8.4.6 Safety & redundancy . . . 62
8.4.7 Requirement assembly & demounting . . . 63

9 Final design . . . 65
9.1 Introduction 65
9.2 Design 65
9.3 Demountable connections 66
9.3.1 Top connection glass column . . . 66
9.3.2 Bottom connection glass column . . . 67
9.3.3 Top connection roof-façade fin . . . 67
9.3.4 Bottom connection façade fin . . . 67
9.4 Detailing 68
9.4.1 Components . . . 68
9.4.2 Component manufacturing . . . 68
9.5 Assembly & demounting 69

V Conclusions & Recommendations

10 Conclusions . . . 75
10.1 Conclusions column in case study context 75
10.1.1 Structural functioning . . . 75
10.1.2 Design aspects . . . 76

10.2 Conclusions column 76

11 Recommendations 79

Bibliography 83

VI Appendices

A Design tensile strength glass 89

B Spring stiffness 91

C Other Diana considerations 93

C.1 Interface modelling considerations 93

D Loading conditions case study 95

D.1 Loading conditions 95

D.1.1 Wind loading 95

D.1.2 Snow loading 96

D.1.3 Variable roof loading 96

D.1.4 Self weight 96

D.1.5 Roof ballast 96

D.2 Governing loading combinations 97

E Load distribution: analytical prediction 99

F Case study design checks 103

F.1 Design checks glass fins 103

F.2 Design checks structural façade 103

F.3 Design checks timber roof 104

G Extra drawings pavilion 105

H Stress concentrations Diana 107

Introduction

1	**Introduction**	3
1.1	Problem statement	
1.2	Research objectives	
1.3	Methodology	
1.4	Report outline	

1. Introduction

1.1 Problem statement

In the past few decades, float glass structures have become increasingly transparent due to the production of larger panels and the design of almost invisible connections. There are numerous examples of structural float glass elements, usually as façade fins or roof beam fins (Figure 1.1). However, load-bearing glass columns remain rare in practice.

(a) (b)

Figure 1.1: The well-known Apple building in New York **(a)**, retrieved from Hauk (2015). An example of a connection detail **(b)**, retrieved from IQ Glass (n.d).

The high compressive strength of the material glass in combination with its transparency, make it an attractive material to use for a column. The brittle failure behaviour of glass however poses a challenge and requires extra attention during the design phase to ensure a safe structure with sufficient redundancy.

Various types and configurations of glass columns have been subject of academic research. However, a demountable glass column made from laminated components remains unexplored. This structural concept allows for modular and temporary structures with incorporated structural safety. A similar concept, using interlocking cast glass geometry, has been investigated in small scale research as a construction method for a wall or bridge deck. However, a column made of interlocking components remains relatively unexplored. Interlocking laminated elements have not yet been explored at all.

Below is a list of advantages of using interlocking, laminated glass components as a construction method for a column:

- Allows for modular and temporary structures that can be re-used
- Quicker assembly than when using a (UV curing) adhesive
- Replacing smaller, damaged components is economically advantageous
- Less time consuming to produce than cast glass elements
- Form freedom resulting from water jet cutting
- Incorporated safety due to lamination
- Redundancy because of small components
- Aesthetically appealing design with openings between elements

This construction method however does bring about stability challenges. A comprehensive understanding of the structural behaviour of such a column is necessary before application in the built environment is possible. Thus far, a numerical analysis has not been conducted on columns made up of interlocking laminated elements, while this analysis can help understand the stability, force distribution and stress concentrations of such a system. Furthermore, there are almost endless design possibilities for this new concept. Material and fabrication constraints need to be investigated, as well as ideal column dimensions.

In order to investigate the feasibility of such a structural design concept, a case study is introduced (Figure 1.2) to give context and boundary conditions for the column. The glass column stands in the middle of the pavilion and helps support the roof. This way it is the central, eye-catching feature of the pavilion. The small, temporary pavilion will travel through the Netherlands. It has a floor space of 10 by 10 meters. Pavilions are an ideal type of structure to experiment with building innovations because of limited regulations and low costs. The case study is further discussed in Part IV.

(a) (b)

Figure 1.2: The pavilion in (**a**) and an exploded view of the laminated glass components that make up the column in (**b**).

1.2 Research objectives

The main objective of this research is to obtain a feasible all-glass column design by providing a stable structure and by predicting and preventing tensile peak stresses using Finite Element Analysis. Different parameters will be investigated in order to obtain a column design that contributes best to taking up different loads. Extensive design trade-offs will be discussed and visualised. Material and fabrication constraints will be considered, along with aesthetics in order to provide a well-considered overall design. More general conclusions can be drawn from this research, which can serve as guidelines or recommendations for similar conceptual designs.

The main research question of this thesis reads:

> What structural parameters are governing in the design of a demountable column made up of interlocking, laminated glass components?

To answer this question, the following sub questions are formulated:
- Can the column play a significant role in stabilising a structure, i.e. how does the column take up horizontal loading?
- How do the (dimensions of the) interlocking components influence the stability, load bearing capacity and stress concentrations of the column?
- How does the secondary support structure influence and guarantee that displacements and stresses remain within the limits stated by the Eurocode?

The following sub questions are formulated concerning this specific case study:
- How are the roof-column and column-foundation loads transferred?
- How is redundancy incorporated into the design of the pavilion to guarantee a safe design?
- How will the pavilion be assembled and demounted?

1.3 Methodology

To answer the research questions, the methodology as visualised in Figure 1.3 is used. The conceptual design of a demountable, laminated glass column has not previously been investigated. In order to accomplish a feasible design, a variety of relevant structural parameters and design aspects is investigated. Initially, existing literature is consulted regarding the material glass and to gain understanding of challenges in previously built or researched glass structures. Based on these insights, a column design is proposed after which analytical predictions are set up. These will serve as a reference check for the later conducted numerical calculations by means of Finite Element Analysis (FEA). Furthermore, the FEA input is carefully considered and motivated. The outcome of this FEA can therefore be judged as valid as applied in this research. It is subsequently used to iterate and adapt the column design.

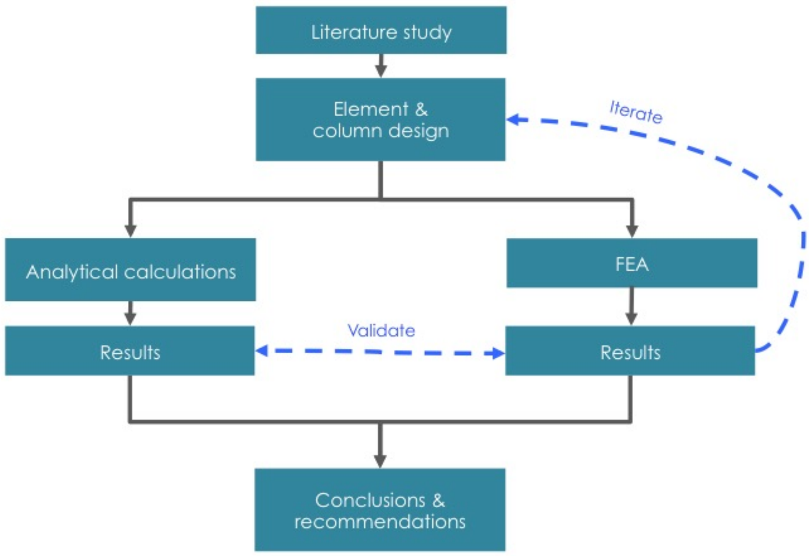

Figure 1.3: Methodology used for this research.

The physical nonlinear behaviour of the interlayers, along with geometric nonlinearities, make linear (analytical) analyses insufficient for accurately predicting the structural behaviour of a column using this construction method. However, analytical predictions can serve as upper bound solution and are useful to compare the FE outcomes with. FEA is able to account for nonlinearities and makes it possible to test different parameter variations relatively easily. By visualising loads, displacements and stress concentrations, the Finite Element (FE) model can be used as an iterative design tool to obtain a feasible design for this novel type of column. The software program Diana has been selected because of available expertise at the university.

Physical laboratory experiments would be another way to approach this research. However, this is a very time-consuming and expensive method. Material properties of laminated glass are well documented in existing literature, so these can be used as reliable input for the FE model. The outcome of this research can be compared to the results of physical experiments conducted in the future.

Before physical specimens for laboratory testing can be produced, different production possibilities need to be considered. In this research, material and design constraints and limitations will be identified and traded-off against one another, presenting a feasible and aesthetic design.

1.4 Report outline

Figure 1.4 gives an overview of the report structure.

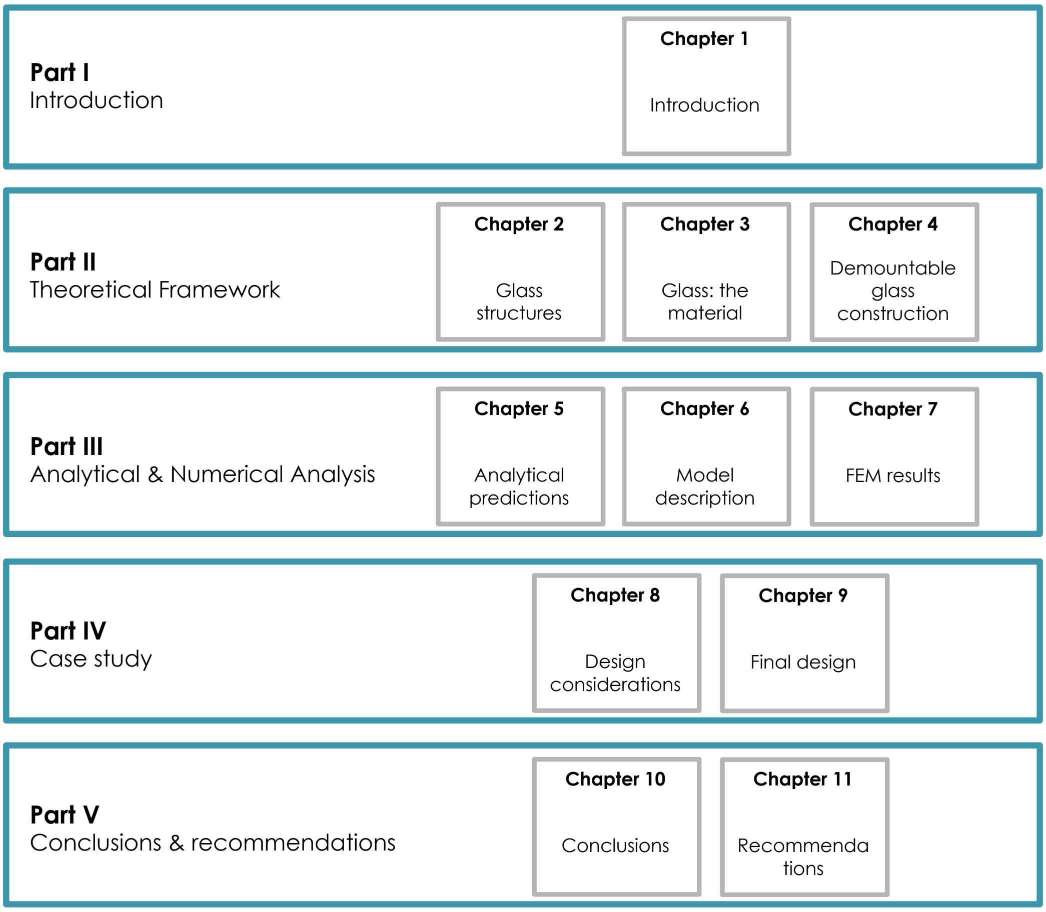

Figure 1.4: The outline of the report.

Theoretical Framework

2 Glass structures 11
2.1 Introduction
2.2 Glass columns
2.3 Glass building envelopes

3 Glass: the material 19
3.1 Introduction
3.2 Production process
3.3 Post processing
3.4 Heat treatment
3.5 Lamination
3.6 Material properties
3.7 Safety and design
3.8 Recycling and sustainability

4 Demountable glass construction . . 27
4.1 Introduction
4.2 Interlocking mechanisms glass
4.3 Dry interlayers
4.4 Boundary conditions interlocking structures
4.5 Conclusions demountable glass construction

2. Glass structures

2.1 Introduction

Glass is not commonly used as a load bearing material, though there are examples where this is the case. This chapter gives an overview of the research field and the application of load bearing glass structures.

2.2 Glass columns

Glass columns could be a solution to realise visually continuous space. The material can take up large compressive loads and therefore lends itself for the fabrication of a column. Glass columns have mainly been the topic of academic research and there are limited examples of application in buildings. Nijsse and ten Brincke (2014) defined five categories of all-glass columns (Figure 2.1), namely: profile, layered tubular, stacked, bundled and cast. These five types of glass columns will be covered in the following sub-sections.

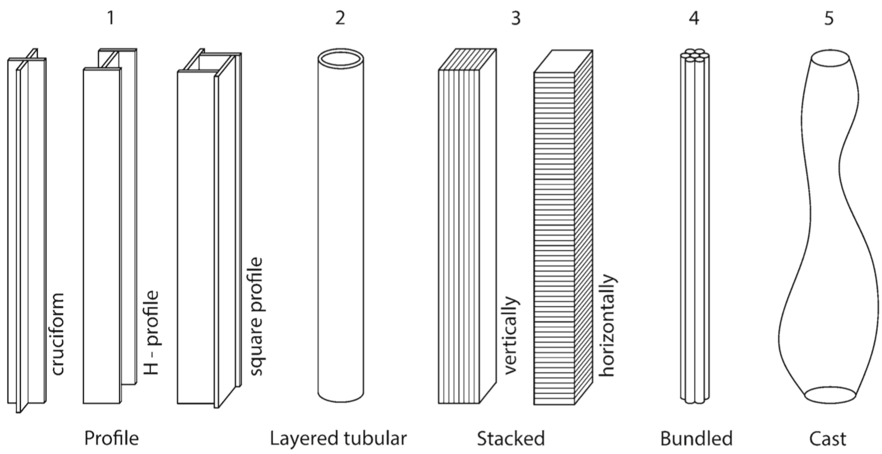

Figure 2.1: The 5 types of glass columns as classified by Nijsse & ten Brincke (2014).

2.2.1 Profiled glass column

Profiled glass columns are made up of rectangular flat panels connected by means of a transparent adhesive. There are various possible configurations such as: cruciform, H-profile or square profile.

Profiled glass columns are the only glass columns that have been applied in practice. To the author's knowledge there are three examples where profiled columns have been realised in buildings, all of which are cruciform. These projects are: the town hall in St-Germain-en-Laye, France (1994); a coffee house in Göppingen, Germany (2006) and the Danfoss headquarters in Nordborg, Denmark (2009). Examples of the appearance of these columns can be seen in Figure 2.2.

(a) **(b)**

Figure 2.2: Images of the glass columns in St-Germain-en-Laye **(a)** taken from Karmatrendz (n.d.) and Nordborg **(b)** taken from Bagger (n.d.).

The configuration of the layered glass panels varies slightly. As depicted in Figure 2.3, the structural layers of the columns in St-Germain-en-Laye are interrupted, while these remain uninterrupted in the other two examples. The columns of the Danfoss headquarters in Nordborg are the most transparent because low-iron glass was used (Figure 2.2b). Structural redundancy has been implemented in the roof design to guarantee a safe design.

Ouwerkerk (2011) identified a few parameters that influence the strength of profiled glass columns. Difference in vertical position of the assembled glass plates and imperfections at the top and bottom edges reduce the strength of this type of column.

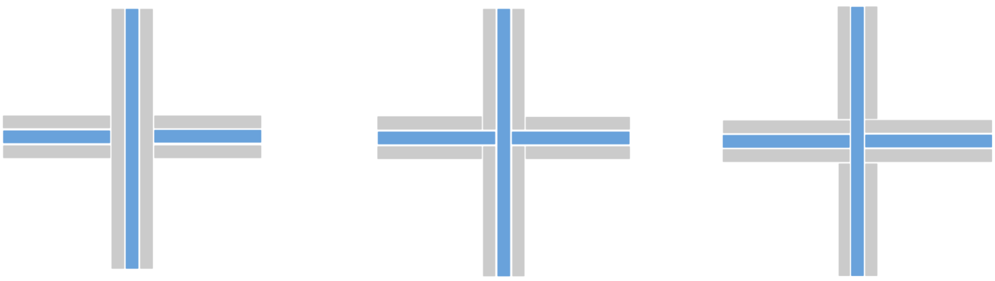

Figure 2.3: Different configurations of cruciform profiled glass columns in: St-Germain-en-Laye (left), Göppingen (middle) and Nordborg (right). Adapted image taken from Heugten (2013).

2.2.2 Layered tubular column

Layered tubular columns are made up of two concentric glass tubes with one smaller tube sliding into the tube with the larger diameter. These are laminated together by (UV curing) resin. The result is a very transparent design that slightly distorts what is behind it (Figure 2.4). Dimensional intolerances of the glass tubes as well as shrinkage of the adhesive make it challenging to obtain consistent results (Nieuwenhuijzen, Bos & Veer, 2005).

(a) **(b)**

Figure 2.4: The tubular glass column in the TU Delft laboratory **(a)** and the slight distortion of the tubular column **(b)** both retrieved from Veer & Pastunink (1999).

2.2.3 Stacked column

Layers of glass can be stacked either horizontally or vertically to form a column (type 3 of Figure 2.1). Differently shaped layers can be stacked on top of each other, allowing for a high degree of form freedom. There are artists who use this principle to make sculptures (Figure 2.5); often the plates are glued together with an adhesive. The drawback of stacked glass however, is that it is not transparent from all angles. There are different methods to connect the layers, namely: lamination, adhesive, mechanical connection or superimposed load. Generally, when more than five layers are stacked, an adhesive is used and not lamination. Lamination is quicker and guarantees high quality.

Stacked columns require small tolerances for successful functioning. Uneven surfaces may cause stress concentrations at the contact points, leading to lower load bearing capacity. Heugten (2013) mentioned three aspects important to prevent premature failure, namely: minimising differences in glass thickness, limiting bow and reducing the presence of roller waves. Heugten (2013) investigated several types of adhesive films and liquid adhesives for bonding the glass plates together. The liquid adhesive AD821 proved to be most promising because the column best resembled monolithic behaviour and presented the least sudden failure behaviour.

(a)

(b)

Figure 2.5: The glass sphinx sculpture in **(a)**, image taken from Omroep Venlo (2015). The glass angel sculpture in **(b)**, taken from Sim (2011).

2.2.4 Bundled column

The bundled column was designed in 2000 for the lobby of ABT's head office in Velp, the Netherlands. The column consisted 7 identical solid glass rods, where six glass rods were configured around a circular central rod. This column was never realised because test results were not consistent for either the visual and structural performance (Oikonomopoulou, van den Broek, Bristogianni, Veer & Nijsse, 2017).

Oikonomopoulou, van den Broek, et al. (2017) investigated a configuration where six rods encircle a central star-shaped rod (Figure 2.6a). To ensure proper coupling of the rods, the curvature of the central and outer rods needs to match. Also using an appropriate adhesive is important. In order for the conducted tests to be economically feasible, only standard available profiles were used. Rods up to 1500mm in length were stacked vertically to obtain a real life size column. Three types of connections were investigated, namely: a gap between the glass rods, an adhesive connection or a thin aluminium ring connection. The aluminium ring proved to approximate monolithic behaviour the best. Also post-tensioning was investigated in order to obtain more gradual failure behaviour. These post tensioned bundled glass elements were applied as truss elements for the bridge at the TU Delft campus (Figure 2.6b). The steel deck will be replaced by a glass one consisting of interlocking cast components at a later stage.

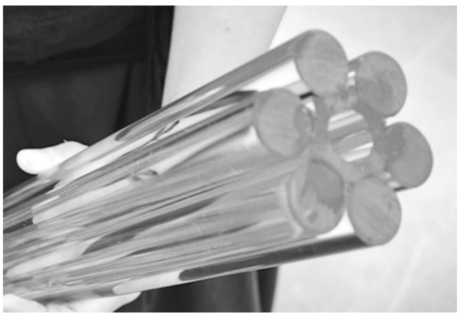

(a)

(b)

Figure 2.6: An example of a bundled column with a star shaped centre profile **(a)** retrieved from Oikonomopoulou, van den Broek, et al. (2017) and the glass truss elements used for the bridge at the TU Delft campus **(b)** retrieved from Schott (n.d.).

2.2.5 Cast column

The render of the envisioned Danteum monument in Figure 2.7 illustrates a multitude of cast glass columns. These could be the solution for transparent columns in almost any desired shape. Producing such a column would however require a long and controlled cooling process, making it an expensive solution. Also, large cast elements would be costly to replace if damaged.

Although academic research on a monolithic cast column has not taken place, columns made up of smaller cast elements have been investigated. Felekou (2016) investigated a column made up of cast glass brick components bonded by a UV-curing adhesive. This column was compared to a stacked column (type 3 in Figure 2.1) and proved to be stronger and stiffer because of thicker elements. Akerboom (2016) investigated a column consisting of circular interlocking components with dry interlayers in between. It was concluded that failure occured due to poor end connections, making it difficult to accurately determine the strength of the column.

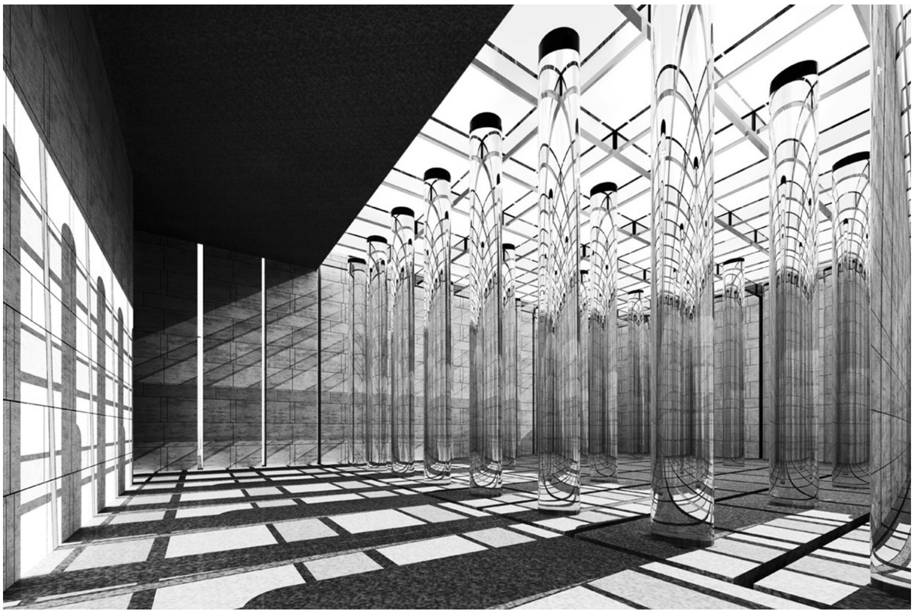

Figure 2.7: A rendering of cast glass columns in the conceptualisation of Danteum ("The Danteum", n.d.).

2.2.6 End connections

Many glass columns have undergone physical testing in order to determine their axial compressive capacity. However, the research field pays little attention to end connections of columns as a separate topic. There is however some literature that covers this subject. Both physical experiments and design concepts are discussed. Boundary conditions for interlocking columns will be discussed in Section 4.4.

Ouwerkerk (2011) investigated two differently executed end connections for H-shaped profiled columns. For the set up in Figure 2.8a, the steel was glued to the flanges of the column with epoxy Araldite. The other configuration (Figure 2.8b) used polyurethane rubber which was cast between the steel shoe and glass. This connection functioned more poorly than the first one, presumably because the rubber was either not thick enough or unsuitable as a material. Also more importantly, the first configuration avoids force transfer via the edges of the glass, preventing stress concentrations caused by imperfections. The connection was translated to the design proposal in Figure 2.8c.

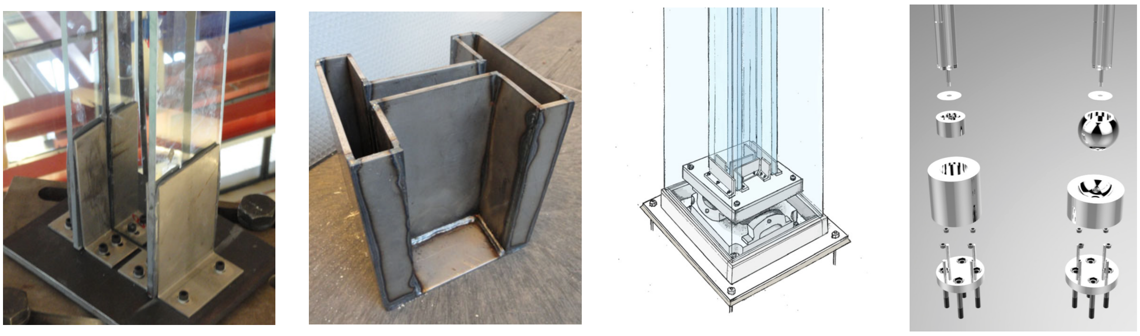

(a) (b) (c) (d)

Figure 2.8: The test specimens by Ouwerkerk (2011) for two types of end connections can be seen in **(a)** and **(b)**. The subsequent archictural concept by Ouwerkerk (2011) can be seen in **(c)**. A concept for a bundled column end connection by van den Broek (2016) is illustrated in **(d)**.

A real-life example of executed end connections for profiled columns can be seen in Figure 2.2. For the Danfoss headquarters (Figure 2.2b) a 10mm thick neoprene strip was placed between the glass and steel shoe (Petersen & Bagger, 2009). The detail allows for rotation and thus prevents the column from having to take up bending moment.

Oikonomopoulou, van den Broek, et al. (2017) tested both pinned and clamped end connections for a bundled column. After testing it however turned out that the clamped connection resembled a connection in between pinned and clamped. An architectural proposal for a clamped and pinned connection for a bundled column as proposed by van den Broek (2016) is displayed in Figure 2.8d.

2.2.7 Comparison glass columns

Of the different types of glass columns presented in literature, the least research has been done on cast and stacked columns (type 3 and 5 from Figure 2.1). Other types of glass columns are also possible, as are hybrid solutions of the previously mentioned types, for example columns made up of stacked cast elements. Choosing a suitable column depends on many aspects such as design brief and desired aesthetic appearance. The different types of columns are compared in Table 2.1. The first five columns of Table 2.1 are the types of columns discussed in existing literature and are displayed in Figure 2.1. The final column has not yet been researched and is made from interlocking laminated components with the use of a dry interlayer instead of an adhesive (Figure 1.2b).

Table 2.1: Comparison glass columns

	Profiled	**Tubular**	**Stacked**	**Bundled**	**Cast**	**Interlocking laminated components**
Compressive strength	+	++	+	+-	Unknown	Unknown
Transparency	+	++	- -	+	++	+-
Safety	+	+	++	+	+-	+
Fabrication ease	+	- -	+	+	+	+
Fabrication time	+	+	-	+	- -	+-
Form freedom	-	-	++	-	++	+
Efficient material use	+	+	-	+	-	+-
Low costs	+	+	-	+	- -	+-
Demount-ability	-	-	-	-	-	++
Total	**+**	**+**	**-**	**+-**	**-**	**++**

2.3 Glass building envelopes

Oikonomopoulou et al. (2018) mentioned three different design concepts for self-supporting building envelopes made from cast glass components, which are depicted in Figure 2.9. These concepts can also be applied for other structural elements, such as columns or arches. The first approach uses an additional metal substructure to take up tensile forces. This substructure is visible through the glass elements. The second method bonds glass elements together using an adhesive. The downside to this technique is that it is not reversible. Lastly, interlocking cast elements with dry interlayers are a reversible construction concept. Example buildings from each category will shortly be illustrated in the following subsections.

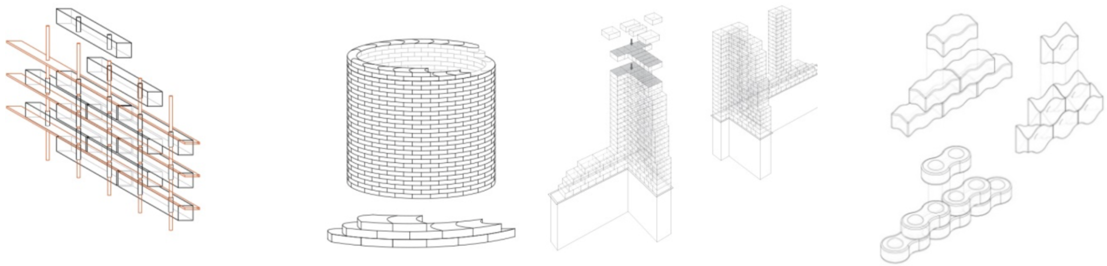

Figure 2.9: The three different design concepts for self-supporting building envelopes. Note: the middle two images belong to the same design concept. Left: metal substructure, middle: glued elements and right: interlocking elements. Image taken from Oikonomopoulou et al. (2018).

2.3.1 Building envelopes with metal substructure

The Optical House in Hiroshima, Japan was constructed in 2012 and is illustrated in Figure 2.10a. This façade is made up of 6000 glass bricks through which metal rods run vertically. Every two layers a horizontal flat steel bar is strung between the glass elements to withstand lateral loading, which can be seen in Figure 2.10b. The façade is extremely slender, only 50mm thick while it is 8.6m high. This is possible because the façade is suspended from a pre-tensioned composite steel-concrete beam.

(a) **(b)**

Figure 2.10: The façade of Optical House **(a)** taken from ("Optical House", n.d.) and construction **(b)** taken from ("Optical House construction", n.d.).

Crown Fountain was constructed in Chicago in 2009 and also used an additional metal substructure, though slightly differently from Optical House. An internal stainless steel frame was used to support its self-weight and provide resistance against wind loading.

2.3.2 Building envelopes with adhesively bonded elements

The Crystal House (2016) in Amsterdam is an innovative, load-bearing façade constructed with glass bricks glued together using a UV curing adhesive (Figure 2.11). In order to minimise the visual impact, glue was used with roughly the same refractive index as glass. The applied glue layer needed to be very thin in order to be strong and transparent enough. Therefore the adhesive could not compensate for large defects or tolerances in the bricks, making it necessary for them to be fabricated with a precision of about 0,25mm. Laboratory tests conducted by Oikonomopoulou, Bristogianni, et al. (2017) proved monolithic behaviour of the adhesively bonded elements. No suitable glue was found to bond the glass to the terracotta bricks. As a solution brown ceramic strips were glued to the front of the glass bricks to give the illusion of a gradient.

The drawback of this construction method is that it is very time consuming. The bricks needed an annealing time of 36-38 hours and precisely gluing them together using a UV light is a tedious task. About a year after construction completed, cracks developed in the glued joints. Despite this, the structure is still deemed safe.

(a) (b)

Figure 2.11: The façade of the Crystal House in Amsterdam can look almost transparent **(a)** or mirror the sky **(b)**, depending on weather conditions and viewing point. Images both retrieved from MVRDV (2016).

2.3.3 Building envelopes using interlocking geometry

Interlocking cast glass elements have been proposed as architectural concepts for historic monument consolidation by both Barou (2016) and Jacobs (2017) (Figure 4.2a and 4.2c). Neither of these have been brought into practice. The greatest advantage is that this technique is reversible, in theory at least. In practice some sort of starting point or connection is needed between the glass elements and existing building or ruin. This usually requires some sort of drilling or mechanical fastening, making it not completely reversible. Provided there are boundary conditions which restrain the geometry, this method can be completely self supporting. More on interlocking geometry can be found in Chapter 4.2.

3. Glass: the material

3.1 Introduction

Glass is a remarkable material because it is transparent: it is made of non-transparent raw materials such as silica, sand and limestone that are combined and heated to form a transparent durable but fragile material. This chapter summarised the background of the behaviour and constraints of the material glass.

3.2 Production process

There are numerous types of glass production processes depending on the final product or the end application, but all the manufacturing methods require that the raw materials are combined and heated to very high temperatures, when glass is semi solid, and subsequently cools to the solid state.

Glass elements are manufactured using one of the following production methods: float, cast or extruded. The float glass method is the most widely used production method for glass. The basic principle remains unchanged since it's invention, but it has become highly automated since then, allowing for mass production and high accuracy. The main advantages of this technique are its consistently high optical quality and low costs.

In Figure 3.1 the production method of float glass is visualised. After the raw materials are molten they continue to a tin bath where the mixture floats on the tin and forms a thin layer of glass. This solid ribbon continues to the annealing lehr where it cools down in a controlled manner to prevent residual stresses. After automatic inspection the glass is ready to be cut and undergo further treatment. Float glass is usually cut to the international ribbon size of 3.21 x 6.0m (Weller, Harth, Tasche & Unnewehr, 2009). The width is limited by the float glass plant and the length has to do with transportation constraints. In China larger panels are produced with a lengths up to 25m. However, this does lead to significantly higher production costs and on top of that special transportation is needed to get these large panels to site.

Casting glass starts off by pouring molten glass into a mould. This technique allows for form freedom because the mould can be made into any desired shape. There is a slight difference between hot pouring and kiln casting. During kiln casting the mould is in the kiln during the entire process; solid glass pieces and take the shape of the mould. During hot pouring the mould does not go into the kiln until after pouring. When the molten glass in the mould has cooled off to about 750°C, the glass is taken out of the mould and put into the kiln. The hot pouring method was used to make the glass bricks for the Crystal House in Amsterdam mentioned in Section 2.3.2.

Extrusion is used to make rod-like glass elements with a homogeneously shaped cross section. All sorts of shapes and sizes are possible such as: hollow or solid, circular, triangular, ribbed, smooth, star-shaped or otherwise. Extrusion results in cross sections with precise tolerances, though the rods can present a bowed shape instead of being completely straight. This production method was used for the individual rods of the bundled glass column described in Chapter 2.2.4.

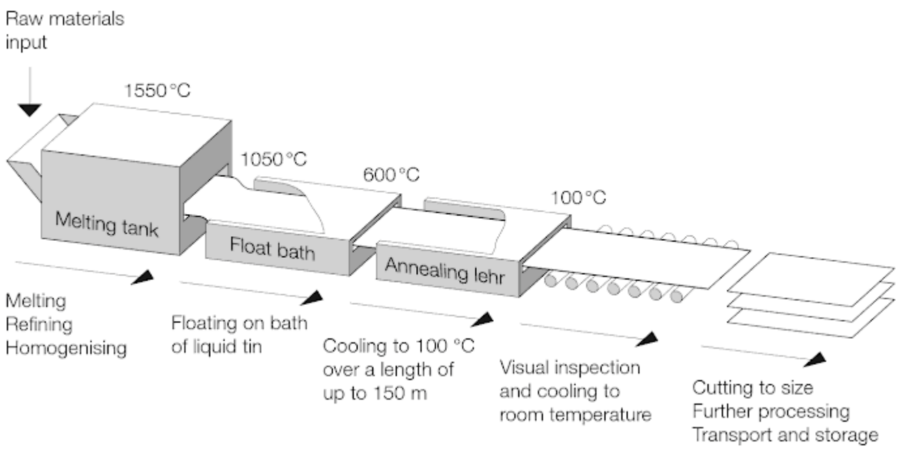

Figure 3.1: Schematic image of a float line (Weller et al., 2009).

3.3 Post processing

After float glass comes off the production line, it can be cut into the desired shape. Edges are then ground and polished to remove small chips and damages. When float glass is water jet cut, this post processing is not necessary because it does not damage the glass as much as cutting does. There are many other post processing possibilities that can be applied to meet specific needs of a designer or client. Patterns can be etched on the glass for aesthetic reasons. Also, hot or cold bending can be applied to make curved panels. There are also many types of coating available that can increase its insulating performance.

Cast glass commonly needs some sort of post processing to remove irregularities caused by the production process. Polishing can be done to smooth and flatten the surfaces; this can be manually or mechanically with a CNC for example. Post processing will significantly increase the costs. It depends on the design constraints whether or not post processing is necessary. For example, the Crystal House required post processing because the allowable tolerances were stricter than could be achieved by the casting process.

3.4 Heat treatment

Annealed glass is another term for float glass. Letting glass cool down in a controlled manner (i.e. annealing) prevents residual stresses in the glass.

Heat-treated glass purposely introduces residual stresses in the glass by reheating the pane of glass and letting it cool down rapidly. This way the glass is pre-stressed: the outer part of the cross section is in compression while the inner part is in tension. When the glass is in tension the residual compressive stresses need to be overcome first, leading to higher tensile capacity. This way surface flaws are less likely to propagate and cause cracks (Figure 3.4).

There are two different types of heat-treated glass: heat strengthened glass and fully tempered glass. The basic principle is the same, but the level of pre-stressing differs. Fully tempered glass has a higher level of pre-stressing due to faster cooling, resulting in a higher tensile strength than heat strengthened glass (Table 3.1).

Furthermore, the breakage pattern of these types of glass is different. Annealed glass breaks into large pieces. Fully tempered glass shatters into small fragments but has no bearing capacity left after breaking. The advantage of heat-strengthened glass is that it retains some load bearing capacity after breakage. This trade-off is depicted in Figure 3.2. The temperature differential for the types of glass varies; Float glass can withstand temperature differential of up to 40 degrees Celsius. Thus, float glass breaks due to (excessive) thermal stresses. Tempered glass can withstand temperature differential of up to 250 degrees Celsius. It has more resistance to thermal stresses.

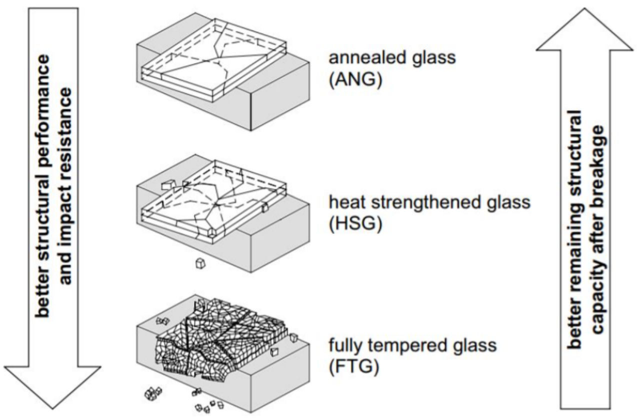

Figure 3.2: Breakage patterns for different methods of heat treatment (Haldimann, Luible & Overend, 2008).

3.5 Lamination

Two or more glass sheets are generally laminated together for safety reasons, preventing breakage into large shards of glass. After placing a foil between the glass panes, heat and pressure are applied in an autoclave. The most commonly used foils are: polyvinyl butryal (PVB), ethylene-vinyl acetate (EVA) and SGP (DuPont's Sentryglas). Generally, PVB is more susceptible to moisture than EVA, which can lead to delamination. SGP is the stiffest and was originally developed for hurricane prone areas.

Generally the size of the autoclave and transportation dimensions limit the size of laminated panels. Currently, the largest panels are produced in China, with dimensions up to 25m in length. Figure

3.3 shows the lamination of a jumbo plate in a large autoclave.

Usually 2 to 5 panes of glass are laminated together. When more layers are desired an adhesive can be used. For structural elements a thinner pane of glass of 2 to 4mm can be laminated on either side to protect the structural glass layers. This way, only the thin layer breaks and the remainder of the structural element remains in tact.

Figure 3.3: Image of laminating a jumbo plate ("Lamination", n.d.)

3.6 Material properties

Glass has certain properties that make it unique from other materials; these will be discussed below.

3.6.1 Brittle failure

The brittle failure of glass is one of its most distinctive characteristics. It has little ductility, so forces cannot be redistributed. Glass deforms elastically and then fails suddenly and without warning, making it a challenging material to construct load-bearing elements from. Other materials, such as steel, present plastic behaviour, resulting in large deformations that pose as a warning just before failure occurs.

3.6.2 Flaws

Surface and edge flaws influence the failure strength of glass. The production process, post processing and human handling inevitably can cause (microscopic) scratches or cracks, resulting in local peak stresses. The brittleness of glass causes cracks to propagate from these defects and result in premature failure. The most common failure mode in glass is referred to as mode I, which is an opening mode.

Measuring the size and shape of flaws is difficult; therefore, in order to determine the strength of glass, (bending) tests are conducted. Both compressive and tensile stresses arise. The compressive strength of glass is much higher than the flaw reduced tensile strength, meaning that tension stresses will in practice be governing and cause failure.

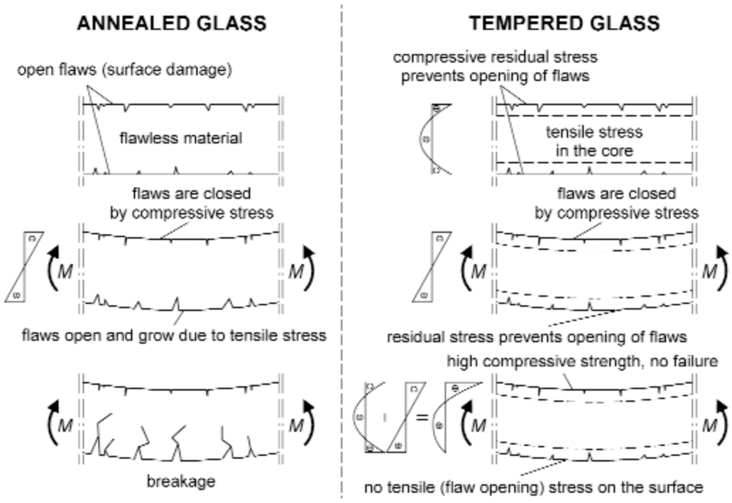

Figure 3.4: Crack propagation for annealed and tempered glass due to surface flaws (EN 1990)

3.6.3 Strength

The theoretical compressive strength of glass is very high, though it is drastically reduced by scratches, inclusions, bubbles or other flaws. Compressive stresses of 200 - 300 MPa are achievable.

Glass resembles the failure behaviour of unreinforced concrete; tensile stresses are governing over compressive stresses and will cause failure. The characteristic tensile bending strength of float glass is 45 MPa. However, the design value is significantly lower and depends on loading conditions, material and safety factors. The maximum allowable value used for this case study is 6,53 MPa, which was defined according to NEN 2608:2014 (Appendix A for exact derivation).

Heat treated glass is stronger than annealing glass. Heat strengthened glass has a characteritic bending strength of 70 MPa and fully tempered of 120 MPa. A summary is given in Table 3.1.

Table 3.1: Strength of glass per type

Glass type	Characteristic tensile bending strength [MPa]
Annealed glass	45
Heat strengthened glass	70
Fully tempered glass	120

3.7 Safety and design

When designing with structural glass there are a few ways to overcome the drawbacks of glass' brittle nature. Either the glass must retain sufficient bearing capacity after breakage, like cast elements. Otherwise some sort of warning behaviour can be incorporated in the element, for example post tensioning in the previously mentioned bundled column. By ensuring redistribution of forces, the structure will still take up the applied load despite damages to the glass element. In certain circumstances, more conservative safety factors are applied in order to avoid critical loading conditions.

3.7.1 Risks

A commonly used method to quantify risk is the Fine and Kinney method; risk is assessed by predicting the likelihood of occurrence and evaluating possible consequences. NEN 2608:2014 mention acceptable values for risk for structural laminated glass elements. The permissible value depends on the function of the structural element and the function of the building.

3.7.2 Risk reduction

Risk reduction can focus on either reducing the chance of breakage or limiting the consequences when the element does fail. An example of the first strategy is using a sacrificial layer to protect the structural glass layers from breaking. By introducing a secondary load path, the consequences of failure are minimised.

3.7.3 Fire safety for glass

Glass generally has poor fire resistance. This sub chapter will shortly discuss both the regulations and existing solutions to ensure fire safety.

The European standard EN 13501-2 specifies four characteristics that are important for resistance to fire, the first two apply to load bearing elements such as columns. The E, I and W property are applicable to elements with a separation function. The required fire resistance time for load-bearing elements is extensive in order to prevent progressive collapse. However, single storey buildings are exempt from this requirement. The four characteristics mentioned are:

- R Load-bearing capacity: the ability for the element to maintain its strength and stability.
- E Integrity: ability for the element to remain intact.
- I Insulation: ability to keep the unexposed side below 140°C.
- W Radiation: the ability to block heat radiation enough so the non-exposed side remains below 15 kW/m^2 at 1m distance.

For glass partitions or fire resistant doors it is common practice to use an intumescent layer between the glass panes. This gel layer is transparent under regular conditions but expands drastically into white foam when exposed to high temperatures. The outer pane exposed to the fire must fall out first before this gel layer can be activated. The foamed material insulates the glass and protects it from heat, which is in accordance with the above mentioned I property. This layer can protect the neighbouring room against heat and smoke for a desired amount of time. This is between 30 and 120 minutes, depending on the function of the building.

Instead of placing the intumescent material between the glass panes, it is also possible to apply a fire resistant layer on the surface of the glass. A protective layer of transparent Flameguard HCA-TR was investigated and its ability to protect different structural glass beam configurations was evaluated under exposure to 650°C flames. This temperature was chosen to match the intended building use and due to lack of suitable standard fire tests for structural glass. The research concluded that intumescent paint could increase the safety of structural glass for short duration and/or low temperature fires (Veer, van der Voorden, Rijgersberg & Zuidema, 2001). As a reference, a fully developed fire has a temperature of 750°C (Breunese & Maljaars, 2015).

There are also measures to increase the fire resistance of glass according to the E and W principle. Tempered laminated glass or wired glass is used according to the E principle; these types of glass can withstand high temperatures without shattering. Keeping the W principle in mind, it is possible to apply a special coating to resist heat radiation for some time.

3.8 Recycling and sustainability

4TU.Bouw presented the Re^3 strategy, which is "Reduce, Reuse and Recycle" and was formulated specifically for cast elements. However, the philosophy can be applied more widely to glass geometry in general. Reduce refers to using an efficient geometry with limited material. Reuse refers to using multifunctional geometry that can be used for different applications. Recycling should allow for glass to be re-molten in order to make new elements. Current research includes production of new cast elements from lower quality glass containing industrial waste. Though transparency is compromised, this method leads to interesting aesthetic results and still allows for wide spread application.

Laminated glass is mainly used in the building and automotive industry. Though glass is recyclable, end-of-life glass from buildings is rarely recycled for new application (Glass for Europe, 2013). Often laminated glass is disposed of in landfills. In the automotive sector, there has been recent developments for the recycling of laminated wind shields. By means of chemical separation, the PVB layers and the float glass can be separated and both materials can be recycled and reused. The quality of the recycled products is often lower than the initial quality. Crushed glass is often used for other purposes, such as packaging or glass wool (Deloitte, 2016). The amount of energy required (i.e. embodied energy) to make laminated glass can be seen in Table 3.2 and is compared to other building materials.

There is room for more measures to improve the sustainability of (elements made from) laminated glass. Even if the optical quality of the recycled elements is compromised, this could still lead to an interesting visual result, seeing that glass has more qualities than its transparency. Translucency, reflection and refraction can also result in aesthetically interesting outcomes.

Table 3.2: Embodied energy per building material. Values taken from Hammond & Jones (2008) and University of Wellington (n.d.).

Material	Embodied energy [MJ\kg]
Float glass	15,9
Laminated glass	16,3
Structural steel	35
Concrete	1,1
Precast concrete	2
Sawn softwood	7,4
Sawn hardwood	7,8
Glulam timber	12

4. Demountable glass construction

4.1 Introduction

Demountable refers to a temporary and reversible construction method without loss of quality. Demountable construction with glass has not yet been applied, except in research and small scale pioneer projects. It shows potential because of its temporary and reversible character. This chapter will discuss existing interlocking geometries presented in literature for walls and the arched bridge. Background information about related aspects such as dry interlayers and end-connections will also be described.

4.2 Interlocking mechanisms glass

As defined by Oikonomopoulou et al. (2018): "An interlocking system consists of components that employ their geometry to restrain lateral movement in a construction, whereas the whole assembly is stabilized by compressive forces – sometimes, even the self-weight of the construction is sufficient for this purpose." Different interlocking mechanisms for glass are presented in literature, most of which are made from cast glass (Figure 4.1). Generally, these geometries are all made up of identical, repetitive elements or a few different elements that are repeated.

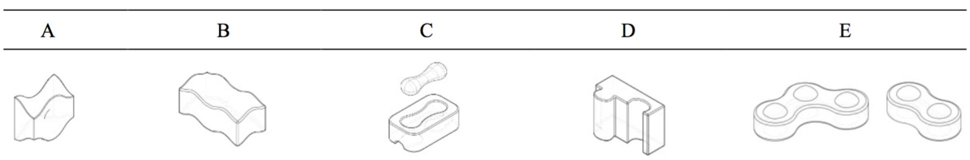

Figure 4.1: Examples of different types of interlocking cast glass geometries defined by Oikonomopoulou et al. (2018).

Some of the design criteria formulated by Oikonomopoulou et al. (2018) are established based on the limitations of casting and therefore would not apply for laminated elements. Firstly, cast elements need a homogeneous mass distribution to prevent inducing residual stresses during the annealing process. Also, the volume of each element should be limited to prevent long annealing time. Annealing times becomes exponentially larger with increasing component dimensions (Oikonomopoulou et al., 2018). However, other specified design criteria are more generic and would apply to interlocking components in general, despite the fabrication method. Examples of this are multi-functionality and constraints in (at least) two directions.

Jacobs (2017) investigated different geometry parameters for cast bricks which form part of an interlocking, dry stacked brick wall (Figure 4.2c). The geometry matches type B in Figure 4.1. A gradually curving interlock was chosen to prevent tensile stress concentrations. Christensen's failure criterion was used to predict failure behaviour, since it takes the brittle nature of glass into account. When comparing Figure 4.2b to 4.2d, it can be seen that the latter has a more gradual stress distribution, making is less susceptible to cracking. Especially the location of the tensile stresses for the Lego-like geometry is not desirable. The interlock is likely to fail under shear and will slide right off. The curved brick is less susceptible to this behaviour. The curvy bricks with a lower structural height failed earlier due to bending, while higher bricks were more susceptible to shear failure.

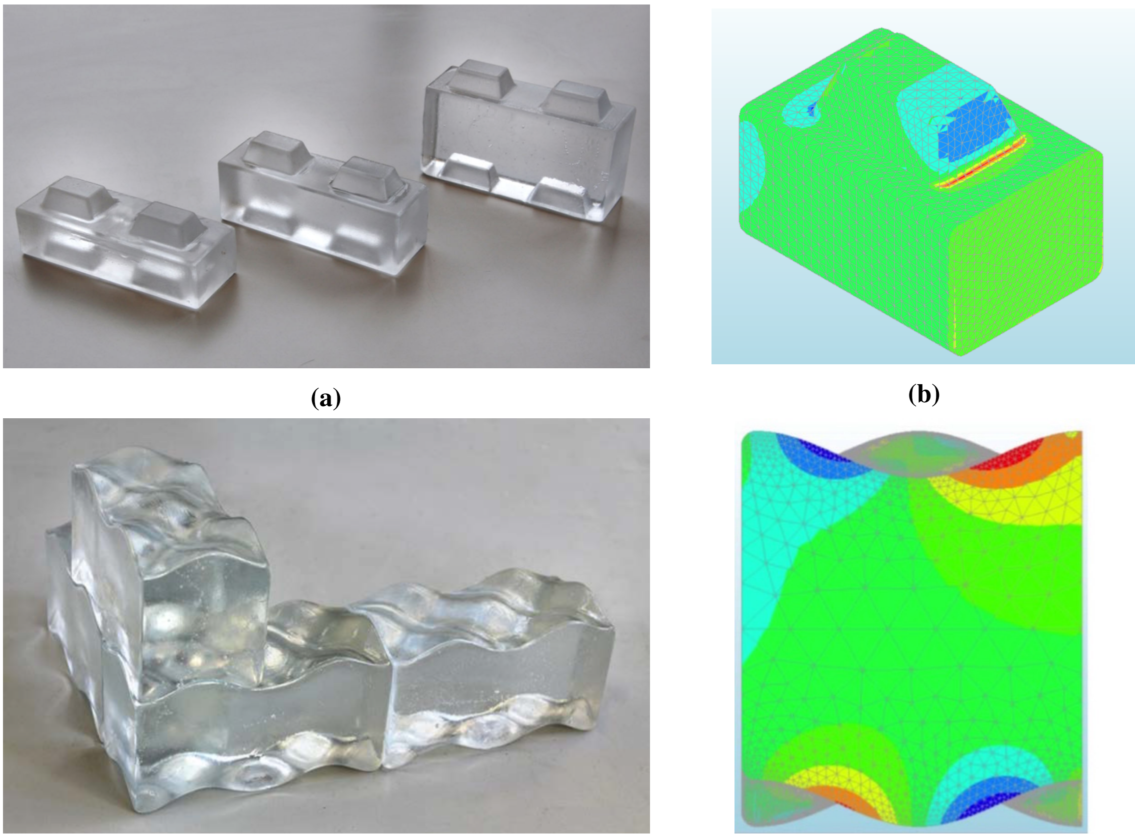

(a) **(b)**

(c) **(d)**

Figure 4.2: Lego like interlocking bricks designed by Barou **(a)**, image taken from Oikonomopoulou, Bristogianni, et al. (2017). FEM analysis done by Jacobs (2017) showing the stress concentrations **(b)**. Curved interlocking bricks **(c)**. Image taken from Oikonomopoulou et al. (2018). FEM analysis showing the stress concentrations **(d)**. Image taken from Jacobs (2017). Red shows tensile peak stresses in the FEM results.

Various research has been done to realise an interlocking deck for the TU Delft campus bridge (Figure 2.6b for an image of the bridge) and different interlocking shapes have been compared. The conclusion was that the brick elements must have rounded or obtuse and chamfered edges. This way molten glass will more easily fill all corners of the mould and damages are less likely to occur to the edges of the completed brick. Three and four point bending tests were conducted to find which of the interlocking mechanisms was best at resisting a combination of shear and bending. The geometry depicted in Figure 4.3a proved to be most suitable (Snijder, Smits, Bristogianni & Nijsse, 2016; Sombroek, 2016). A FE model was created (Aurik, Snijder, Noteboom, Nijsse & Louter, 2018) to compare with the outcome of previously conducted laboratory experiments of a scaled (i.e. smaller) bridge arch. Figure 4.3b illustrates how a point load applied halfway the arch is transferred to the supports by means of compression. The compressive stresses are asymmetric as a result of the component geometry not being mirrored; the rounded part of the components point in the same direction for the entire deck. By visualising stress concentrations, the cracks from the physical experiments can be better understood. Unexpected cracks will most probably be caused by slight surface defects caused by fabrication or handling.

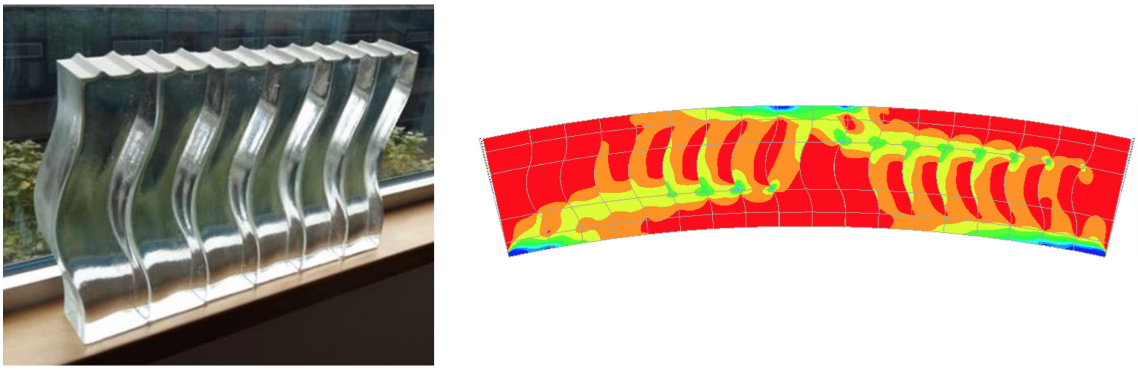

(a) (b)

Figure 4.3: Interlocking brick elements for the TU Delft bridge **(a)** and FEM analysis showing stress concentrations **(b)**. Both images taken from Aurik et al., (2018).

4.3 Dry interlayers

Dry interlayers refer to intermediary material that is not attached to the glass. Unlike adhesives, the glass and interlayer can be easily separated and recycled. Surface imperfections of glass-glass contact result in stress concentrations, which can lead to premature failure. Furthermore, glass-glass has little sliding resistance (Snijder, Veer, et al., 2016). Placing an interlayer in between these glass elements can solve these problems.

Aurik (2017) investigated polyvinyl chloride (PVC) and polyurethane (PU) interlayers of different thicknesses for the arched glass masonry footbridge in Figure 2.6b. These interlayers were made from sheeted material and tested on straight, rectangular glass components. The 1mm thick PVC and 4mm thick PU70 material deemed suitable for the specific bridge case study. However, the modulus of elasticity of the PVC interlayers decreased over time, while the PU interlayers did not display this behaviour. Also PVC discolours to a yellow-ish tint after long exposure to UV light (Oikonomopoulou et al., 2018). Therefore the 4mm PU was finally deemed most suitable out of the tested specimens. Jacobs (2017) used the physical experiments of Aurik (2017) to calibrate the PU material parameters in a FE model.

Both Barou (2016) and Akerboom (2016) used Vivak PETG interlayers because it can be vacuumed into the desired form. The interlayer investigated by Barou (2016) (Figure 4.4b) is difficult to assess because the interlocking mechanism was not fabricated as intended. The cast elements did not have the desired contact surface due to production intolerances, making it difficult to evaluate the interaction between the interlayer and glass. Also, the Vivak interlayer did not have a constant

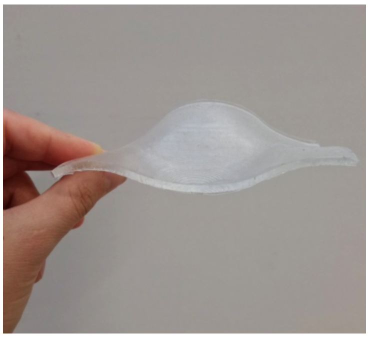

(a)

(b)

Figure 4.4: Cast PU interlayer of 3mm thick **(a)**. Image taken from Oikonomopoulou et al. (2018). An interlayer and its mould that was produced using vacuum thermoforming **(b)**. Image taken from Barou (2017).

thickness. For higher friction, Akerboom (2016) sandblasted the interlayer. The downside is that the interlayer becomes translucent instead of transparent. A proposed solution is to use wet sanding, which results in transparent sheets with higher friction than untreated interlayers.

4.4 Boundary conditions interlocking structures

The aforementioned interlocking mechanisms only function properly when constrained by appropriate boundary conditions. This will be discussed below for different types of structures.

An arched bridge lends itself perfectly for the use of interlocking components. When designed correctly, the complete structure is subject to compression only. This concept dates from ancient times. and was already used by the Romans to construct aqueducts. Stiff enough foundations are a requirement in order for such a bridge to remain stable.

For a wall, interlocking geometry can also be used. The most important requirement is a vertical constraint at the top of the wall to prevent uplifting. This is because bricks at the top are loaded with the least amount of self-weight.

Boundary conditions of an interlocking column are similar to those of a wall; upward lifting should be prevented to avoid instability or collapse. Akerboom (2016) only considered (symmetrical) axial compressive loading and disregarded upward or horizontal loading conditions. The fabricated components failed earlier than expected during laboratory experiment, presumably because of eccentricity and stress concentrations caused by the steel end connections.

4.5 Conclusions demountable glass construction

Laminated interlocking components have not yet been investigated in the literature. However, many lessons learned from interlocking cast elements can be applied to a version using laminated components. For example the interlock should have rounded edges to prevent tensile peak stresses and using repetitive elements is beneficiary for easy production and assembly. Additionally, laminated components do not have some of the design constraints of cast glass, such as limitations on mass distribution and overall size.

III

Analytical & Numerical Analysis

5 **Analytical predictions** 33
5.1 Introduction
5.2 Column buckling
5.3 Bending moment capacity column
5.4 Force distribution

6 **Model description** 39
6.1 Introduction
6.2 Finite Element Model input
6.3 Parameter investigation
6.4 Validity of model

7 **FEM Results** 47
7.1 Introduction
7.2 Stability
7.3 Force distribution
7.4 Stress distribution
7.5 Outcome parameter study

5. Analytical predictions

5.1 Introduction

There are no previously conducted laboratory experiments for a demountable laminated glass column, making it difficult to verify the results of a numeric model. This chapter will present expected behaviour based on simplified analytical calculations. These calculations are linear assumptions and will thus most likely present overly optimistic results. However, these predictions do allow for the numerical results to be put into context and can serve as upper bound reference.

5.2 Column buckling

Below is an analytical derivation of the expected buckling behaviour of the column. This analysis disregards the dry interlayers between the stacked components and assumes a monolithic cross section instead of separately stacked components. Depending on the column geometry and load, buckling may occur due to different reasons, such as eccentric loading or initial out-of-straightness.

The Euler buckling load (Formula 5.1) will be used as an upper bound solution. The end connections will most likely resemble something between clamped and hinged in. The most conservative situation has been chosen, meaning that $l_{\text{cr}} = l$ because hinged end conditions are assumed.

$$F_{cr} = \frac{\pi^2 EI}{l_{cr}^2} \tag{5.1}$$

The deviations of the column geometry depend on the fabrication accuracy of both the glass component and the interlayer. Different configurations can lead to different types of buckling. Traditional water jet cutting can be done with a precision of 0,25 mm. There are also water jet cutters with a precision of 0,12 mm and some are even more accurate. For the 4 mm thick PU interlayer Aurik (2017) measured a standard deviation of 0,10mm, meaning there are also interlayers with larger deviations. Slight deviations in the geometry of both the glass and the PU material can lead to columns with slight irregularities (Figure 5.1).

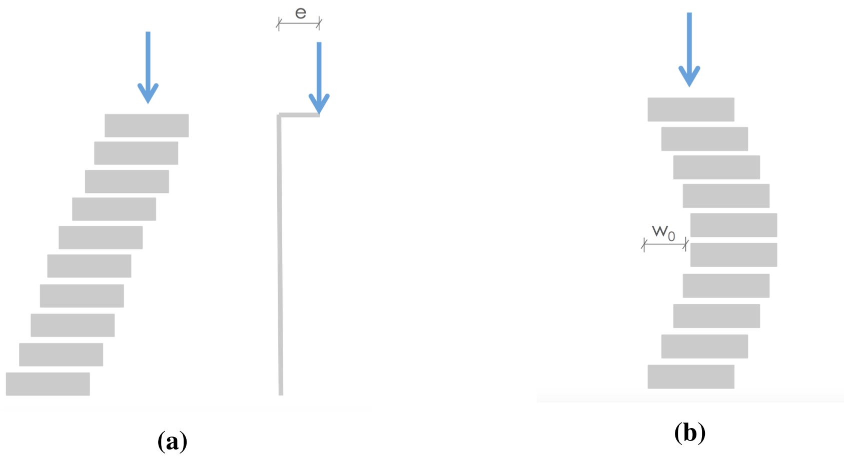

Figure 5.1: Fabrication intolerances of the individual elements can lead to imperfections in the geometry of the column. Buckling due to eccentric loading **(a)** or due to initial out-of-striaghtness **(b)** is possible.

5.2.1 Buckling due to eccentric loading

If considering the most negative situation possible, the column could have an initial eccentricity of 20 mm. This is based on the assumption of 0,25 mm deviation per element plus 0,15 mm deviation per interlayer for 50 stacked layers (Figure 5.1a).

Depending on the precision of fabrication, the initial eccentricity will likely be significantly smaller. The graph in Figure 5.3 shows predicted buckling behaviour. Lateral displacement w is derived using the Formula 5.2, also known as the Secant formula. This formula is derived by solving the differential equation using the appropriate boundary conditions and is therefore an exact solution. The maximum deflection is halfway the column because both end connections are assumed hinged (Figure 5.2). Since there is no initial eccentricity of the column, all values for horizontal displacement start in the origin of the graph.

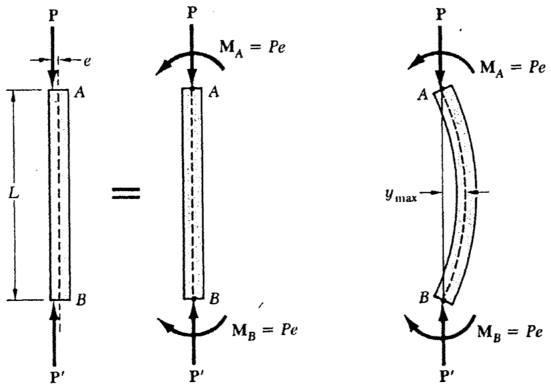

Figure 5.2: Buckling due to eccentric loading. Image taken from University of Washington (n.d.).

$$w = e \times \left[tan\left(\sqrt{\frac{F}{EI}}\frac{L}{2}\right) \times sin\left(\sqrt{\frac{F}{EI}}x\right) + cos\left(\sqrt{\frac{F}{EI}}x\right) - 1 \right] \tag{5.2}$$

The graph in Figure 5.3 shows the expected buckling behaviour according to the Secant formula for different eccentrically applied loads. The Euler buckling load and maximum horizontal

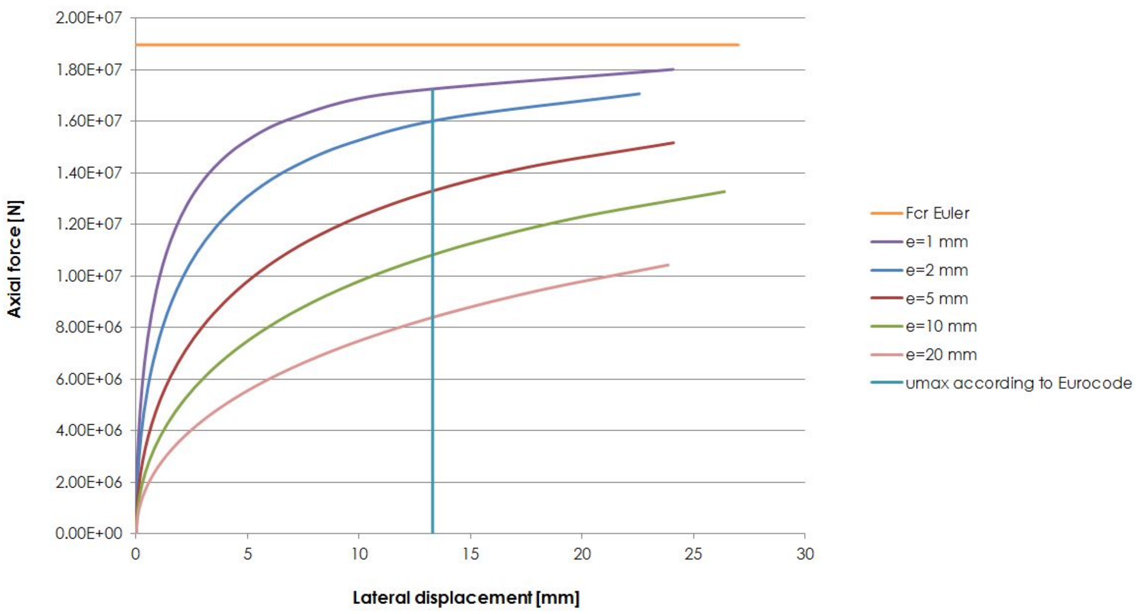

Figure 5.3: Graph showing how eccentric loading influences the buckling load.

displacement as stated by the Eurocode are also displayed in the graph. The maximum compressive load for the defined case study is $1{,}5 \cdot 10^5$. This is far below the permissible load, as can be seen in the graph. It is therefore assumed that the column is safe from buckling caused by eccentric loading for this feasibility study.

5.2.2 Buckling due to initial out-of-straightness

Depending on the method of stacking, another configuration of an imperfect column is possible (Figure 5.1b). The maximum out-of-straightness shape is based on a sinusoidal shape and is largest half way the column. The largest possible initial imperfection is 10 mm, but will most likely be significantly smaller in reality.

The graph in Figure 5.4 displays the predicted buckling behaviour based on a sinusoidal out-of-straightness shape. The initial out-of-straightness can be read on the x-axis. The lateral displacement is determined as followed:

$$w = \frac{n}{n-1} w_0 \qquad with \;\; n = \frac{F_{cr}}{F} \quad (n > 1) \tag{5.3}$$

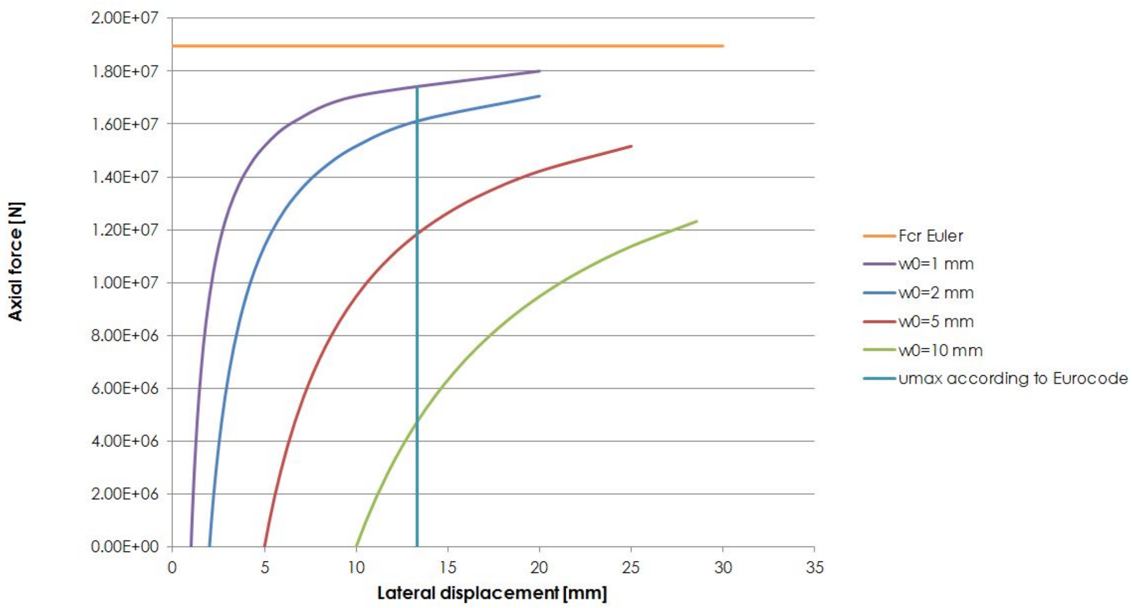

Figure 5.4: Graph displaying how initial out-of-straightness influences the buckling load.

Also for initial out-of-straightness, the analytical prediction shows the case study compressive load is much lower than the buckling load for all investigated lateral displacements.

5.2.3 Conclusions buckling

As can be seen in the graphs, the column is (theoretically) able to take up a very high load before buckling. The influence of initial imperfection and load eccentricity can be seen. The maximum compressive load in the case study is $1{,}5 \cdot 10^5$, and is far below the allowable axial compressive load. In reality the interface elements will drastically reduce the stiffness of the column. The column will most likely become unstable before it presents buckling behaviour. Therefore the axial loading of the column in the case study will be designed to remain far below the Euler buckling in order to ensure safety. This way numerical modelling of buckling behaviour is not necessary. Once the feasibility of the column has been proven under different loading conditions, future research could further investigate to what extent buckling behaviour is relevant for this type of demountable glass column.

5.3 Bending moment capacity column

Figure 5.5 shows how the column can take up bending moment. The top of the image shows a top view of half of the glass column. The blue area is the contact area between the interlocking, laminated glass components. The normal stress σ_N is caused by self-weight or variable loading. The stresses caused horizontal wind loading or by wind suction on the roof, are displayed as σ_M. The stresses combined of σ_N and σ_M must always be in compression, as shown at the bottom of the image. Because the laminated glass components are not mechanically connected to one another, the column is only able to take up as much tension as is applied in the form of compression. When the tensile stresses exceed the applied compression, the column becomes unstable and fails. The red circle in the figure is governing.

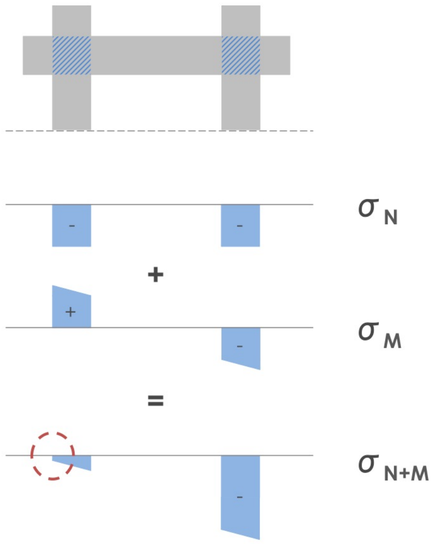

Figure 5.5: Schematic image of column taking up bending moment

5.4 Force distribution

The end-connections of the interlocking column are presumably between clamped and hinged in. This means the column will take up between 0 and 13 % of horizontal loading, as explained in Appendix E. This prediction is based on the assumption that the column is monolithic and has the assigned material properties of glass. How the horizontal forces are distributed between the glass column and façade, also depend on the stiffness of the façade. The stiffer the structural element, the more horizontal load it will attract.

When assuming a monolithic glass column and symmetrical compressive loading, the glass column will take up to 63 % of the total applied load. The column will presumably take up less of the compressive load because the soft interlayer material between each glass component.

6. Model description

6.1 Introduction

The goal of the Finite Element model is to investigate the influence of different column parameters on the stability of the column and structure as a whole. The FEM results are a more accurate representation of reality than the simplified analytical predictions presented in Chapter 5. A detailed description of the model and will be given before presenting the results.

6.2 Finite Element Model input

Below the Finite Element Model as made in Diana is described. Modelling choices are motivated.

6.2.1 Geometry set up

The three dimensional design will be reduced to two dimensional geometry, as is customary when conducting design checks from the Eurocode. The portal frame (Figure 6.2) is a representation of half of the pavilion, meaning the applied loads work over a width of 5m, which is half of the 10m wide pavilion. The portal frame is supported by a spring; the spring represents the structural glass façade that takes up horizontal loading parallel to the portal in another section as would wind bracings (Figure 6.1). Without applying such a spring, the portal becomes unstable; the façade fins are hinged connections and the glass column has a very low stiffness. For the derivation of a realistic spring stiffness see Appendix B. By studying the column as part of a structure, it is put into perspective and context is given. This way the displacements and stresses in the supporting structure can be checked and verified to be realistic.

Different modelling approaches were considered for modelling the separate laminated components. Firstly, using an equivalent thickness for the laminated glass components was considered but proved unnecessary. This is only required when cooperating panes are loaded perpendicularly (Figure 6.3a) and not axially (Figure 6.3b). Furthermore, it is not necessary for short term loading conditions such as wind loading. Therefore an equivalent thickness does not need to be accounted for in the model. Secondly, a layered modelled was not opted for. Laminated glass is a widely used material

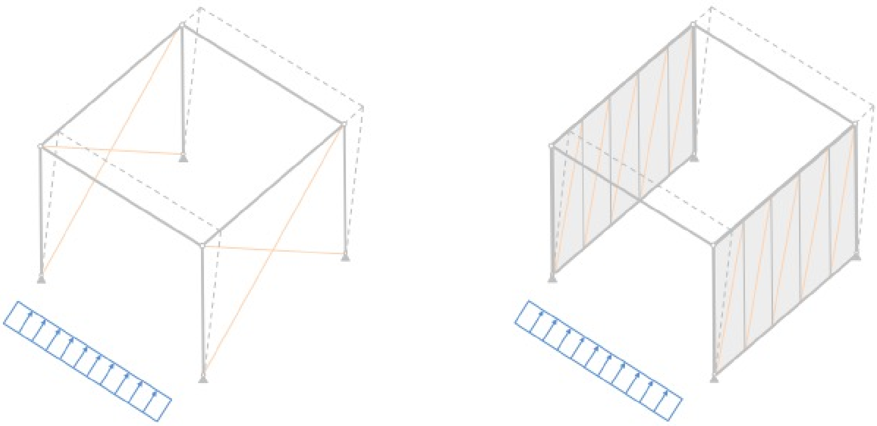

Figure 6.1: Schematic image of wind bracings and structural glass façade panels taking up horizontal wind loading.

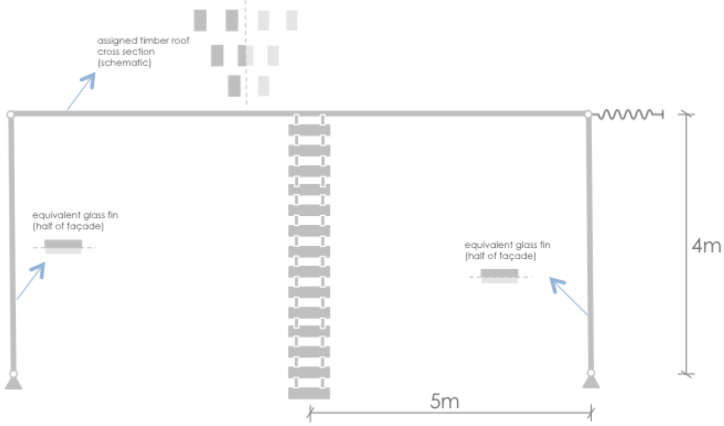

Figure 6.2: Schematic image of geometry input in Diana.

with well documented properties and can be considered to work monolithically. Using a layered model would be unnecessarily complicated. Third, the sacrificial layer is not considered in the FE model because it does not contribute to the strength or stability of the column; its sole purpose is to protect the structural glass layers. Lastly, the choice for the thickness of transversal elements is explained. Diana requires input for the depth of plane stress elements. For the longitudinal elements this is clearly 45mm. However for the transversal elements a variety of dimensions are conceivable. It was opted to choose half of the element length as input for the depth. This parameter barely influenced the results, however larger dimensions resulted in ever so slightly higher stresses, and is thus the conservative approach.

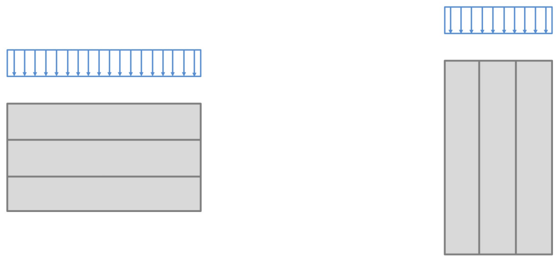

(a) (b)

Figure 6.3: Loading en laminated glass configuration that requires to account for equivalent thickness under certain circumstances **(a)**. The other configuration does not need to take an equivalent thickness into account **(b)**.

6.2.2 Loading conditions

The loading combinations as stated in Appendix D are governing for the pavilion case study. For favourable permanent loads a ULS safety factor of 0.9 is applied, while unfavourable permanent loads are assigned a ULS factor of 1.2. The pavilion will travel through the Netherlands, so the most unfavourable loads have been chosen.

A ballast load of 0,6 kN/m^2 has been chosen because this is the minimum value required in order to prevent uplifting of the roof covering according to Dutch building guidelines. This value is enough to prevent tensile reaction forces in the glass column. A higher ballast load of 1,2 kN/m^2 is also considered.

6.2.3 Model input properties

Below the most important model input will be motivated and explained below. Additional information can be found in Appendix C.

The laminated glass components are modelled as plane stress elements and the interlayers as structural line interface elements which can be seen in Figure 6.4. These element types use linear interpolation. The properties for glass have been modelled according to the values in 6.1; interface properties are shown in Table 6.2.

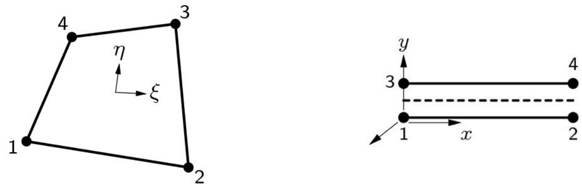

(a) (b)

Figure 6.4: Q8MEM element **(a)** and corresponding interface element L8IF **(b)**. Both taken from Diana FEA (n.d.).

Table 6.1: Assinged linear properties for glass according to NEN-EN 572-1

Assigned properties glass		
Young's modulus	70000	N/mm^2
Poisson's ratio	0,23	-
Mass density	$2{,}5 \cdot 10^{-9}$	T/mm^3

The interlayers between the glass components are modelled as an interface elements in Diana. This type of element is a dummy element, meaning it does not have a certain thickness but rather models the behaviour of the interlayer. This approach was chosen because the interlayer has a very small thickness in comparison to the glass elements; it has previously been used in other numerical models for interlocking glass components (Aurik, 2017; Aurik, et al., 2018).

Choosing a substantiated stiffness for the interfaces is a crucial part of the model. The abbreviation k_n refers to the stiffness in normal direction and k_s refers to the shear stifness of the interface element. There is limited data available from physical testing, meaning the results are not statistically significant. Despite this, the interface stiffness has been based on (limited) existing research. Most important is that the interlayer stiffness is kept constant throughout this research, unless specifically stated otherwise. The properties of the best performing interlayer researched by Aurik (2017) is used as input for this model, namely the 4mm thick PU70 interlayer, which has a Young's Modulus of 137 N/mm^2 according to the literature. Experiments conducted by Aurik (2017) showed E = 336 N/mm^2. However, this value is based on only one test, meaning that conclusions cannot be drawn from this. The results were influenced by interlayer thickness deviations and limited contact area. The value as presented in literature is thus considered more reliable and was chosen as input. This gives the following interlayer stiffness input value:

$$k_n = \frac{137 \quad N/mm^2}{4 \quad mm} = 34 \quad N/mm^3 \tag{6.1}$$

Table 6.2: Assigned interface properties

Assigned interface properties	
k_n	34 N/mm^3
k_s	34 N/mm^3
Interface non-linearities	Discrete cracking
Mode I tension softening criterion	Brittle
Mode II shear criterion	Zero shear traction

The Modified Newton-Raphson (NR) method was chosen as iterative procedure because it led to easier convergence than the Regular NR method. Though the Modified NR method usually needs more iterations, every iteration is faster.

There are two types of nonlinear effects that can be taken into account. The interlayers present physical nonlinear behaviour because they are unable to take up tension. Instead, the elements simply show opening behaviour. This is achieved by applying the settings in Table 6.2. Secondly, geometric nonlinearity is accounted for when required. When only vertical loading is applied, the analysis outcome should not differ significantly for a geometrically linear or nonlinear analysis. However, for horizontal loading it is important to take into account while investigating stability. The Updated Lagrange was chosen as type of geometric nonlinearity. This method uses updated reference geometry while Total Langrange uses un-deformed geometry. Because the loose elements are able to undergo displacements, Updated Lagrange is better suited. Moreover, this method was able to converge relatively easy, while Total Lagrange presented convergence problems for a variety of settings while undergoing horizontal loading. Presumably, this the analysis is unable to attain equilibrium because the displacements of the geometry are not considered.

An additional stop criterion was applied to prevent invalid results. This stopping criteria aborts the analysis when vertical tensile reaction forces larger than 0.001 N occur at the left side of the base of the column such as in Figure 6.5b. Because the elements have no mechanical connection, this behaviour is physically impossible and thus this criterion is assumed to be valid. This stop criterion is not necessary with symmetrical downward loading but is needed when the columns is subjected to wind loading. After applying the stop criterion, the stress distribution and reaction forces of the converged analysis corresponds with Figure 6.5a. In the middle of the base there are small tensile reaction forces. This is only the case with the wider elements and is caused by local behaviour.

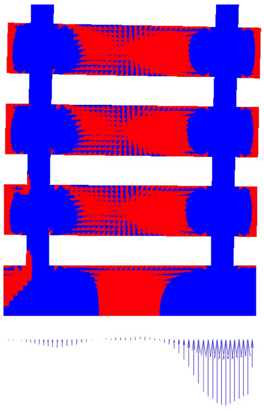

(a)

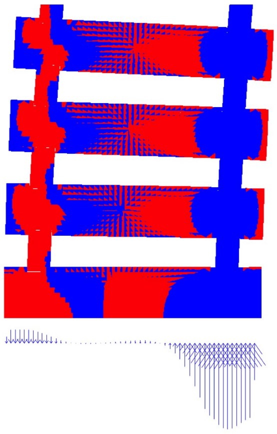

(b)

Figure 6.5: Tensile (red) and compressive stresses (blue) with the corresponding reaction forces. Valid stress distribution in **(a)**; as can be seen there are no downward (= tensile) reaction forces at the left side. An example of invalid reaction forces is shown in **(b)**; significant tensile reaction forces can be seen.

Table 6.3: Assigned properties for other structural elements.

	Area [mm^2]	Moment of inertia [mm^4]	Young's modulus [N/mm^2]
Glass façade fins	9990	$9{,}2315 \cdot 10^7$	70000
Timber roof	110000	$2{,}0056 \cdot 10^{10}$	13700

6.3 Parameter investigation

The influence of the height and width of the glass components on the structural functioning of the column and pavilion will be investigated (Figure 6.6). Also the ballast load, facade stiffness (simplified as k_{spring}) and interlayer thickness will be investigated.

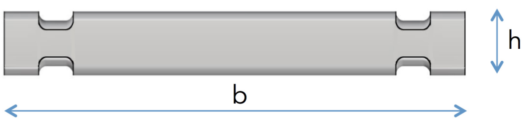

Figure 6.6: Height and width of the laminated glass component will be parameters for investigation

6.4 Validity of model

Before considering the output of the model, the model input is verified with a few checks explained below.

6.4.1 Interface elements

The interface element have been assigned nonlinear properties and should not be unable take up tensile stresses. This nontensile behaviour should go hand-in-hand with opening behaviour of the stacked components.

The stiffness of the interface elements should match the input behaviour (k_n and k_s). This can be checked by dividing the output of the interface tractions (t_n and t_s) by the interface relative displacements (Δ u_n and Δ u_s). This can be done for both the normal direction and shear direction.

$$\frac{t_u \quad [N/mm^2]}{\Delta u_n \qquad [mm]} = k_n \quad [N/mm^3] \tag{6.2}$$

$$\frac{t_s \quad [N/mm^2]}{\Delta u_s \qquad [mm]} = k_s \quad [N/mm^3] \tag{6.3}$$

The relative displacements of the interface elements should be small. The chosen interlayers are 4mm thick, so the displacements should be significantly smaller than this. The experiment conducted by Aurik (2017) shows a deformation of 0.11mm per interlayer under compressive loading. Due to limited data available, this will be used as reference for the maximum allowable relative displacement. However because the interfaces are modelled as dummy interface elements, the relative displacements will likely be smaller.

Finally, the location of compressive stresses in the glass geometry should correspond with the compression in the interlayers. Below are a few images displaying that this is indeed the case.

Two example situations are presented to illustrate the interlayer checks. Figure 6.7a displays the interface stresses for LC1. On the left side interfaces prove to function as desired under tensile loading; they do not present tensile stresses but remain at zero. The right interlayer presents compressive stresses. Parts of the geometry that take up more compression present higher compressive stresses. Note that the normal direction of the vertically oriented interlayers is different from the horizontally oriented parts. Figure 6.7b displays the interlayer behaviour for LC3. The interlayers function the same because loading is symmetrical and present higher tractions due to a higher compressive load than LC1. Both stiffnesses correspond with the input value.

$$k_n = \frac{-0,104102 \quad N/mm^2}{-3,06181 \cdot 10^{-3} \quad mm} = 34,00\, N/mm^3 \qquad k_n = \frac{-3,9194 \quad N/mm^2}{-0,115276 \quad mm} = 34,00\, N/mm^3$$

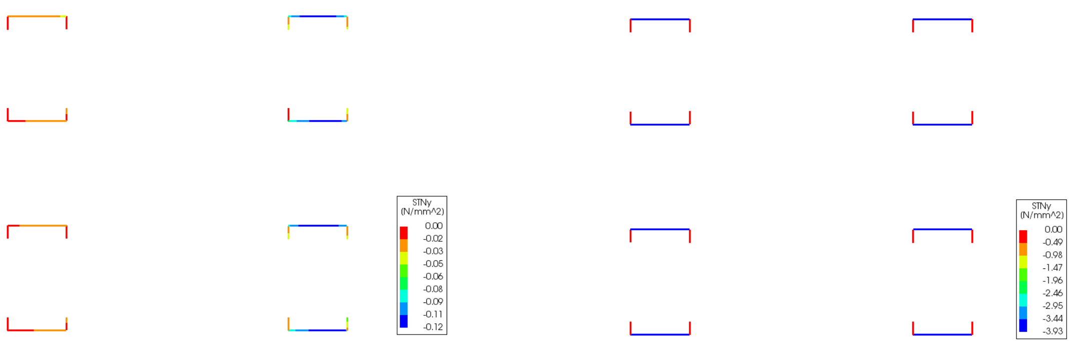

(a) (b)

Figure 6.7: Interface tractions for LC1 **(a)**. Interface tractions for LC3 **(b)**.

6.4.2 Displacements

When carrying out a linear analysis, the displacements of the glass façade fins are the same as expected analytically. The timber roof behaves very stiff, as expected.

6.4.3 Reaction forces

The reaction forces should correspond with the applied load. Small differences between the applied load and reaction forces are permissible and are presumably caused by numeric calculation. The total vertical reaction forces vary slightly for the different dimensioned columns in the parameter study. The different component dimensions result in a slightly different self-weight of the column. This is difference is less than 2% of the total load, depending on the loading combination and applied safety factors. See Table 6.4 for an evaluation of the reaction forces.

Table 6.4: Evaluation reaction forces

		Applied load [N]	Reaction forces [N]	Difference [N]	Difference [%]
LC1	$F_{res,horiz}$	59248	59382	+ 133	+ 0,22 %
	$F_{res,vert}$	2739	2726	- 13	- 0,48 %
LC2	$F_{res,horiz}$	59248	59374	+ 126	+ 0,21%
	$F_{res,vert}$	3241	3234	-7	- 0,22 %
LC3	$F_{res,horiz}$	0	0,00	0	0 %
	$F_{res,vert}$	151408	151385	- 23	- 0,015 %

Also, tensile forces at the base of the column are not allowed because this is not physically possible. The previously explained stopping criterion prevents this, as can be seen Figure 6.5.

7. FEM Results

7.1 Introduction

The results from the Finite Element (FE) model will be explained in this chapter. Firstly, the parameters influencing the stability of the column will be investigated. This is the most pressing issue for this new type of column, because the elements are not mechanically fastened together. Secondly, how much the column contributes to taking up different loads is examined. This determines to what extent this type of column can effectively take up part of the applied loads. Finally, stress distribution and concentrations are inspected and verified to stay within allowable limits. Figure 7.1 is a schematic image to show the different investigated aspects to evaluate the novel type of glass column.

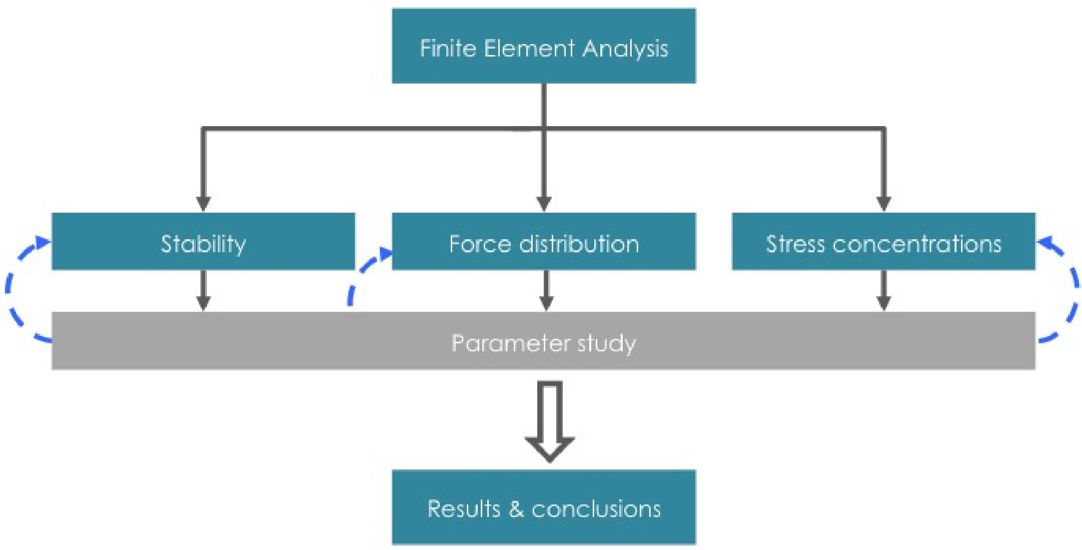

Figure 7.1: A schematic image of the FEA results.

7.2 Stability

The column is considered to be stable when there are no tensile reaction forces at the base of the column, as shown in Figure 6.5. Appropriate safety factors have been applied to both the load and materials, so this is considered to be a safe approach.

Loading combination 1 (LC1) (Appendix D) is most critical in terms stability because of potential uplifting of the roof while there is no mechanical connection between the roof and column; in the FE model this can lead to convergence issues. In real life application this will lead to problems as well, because the unconnected roof will uplift from the column below, which is undesirable. Roof ballast prevents this uplifting behaviour caused by wind suction. Since this is a stability matter, the ULS safety factor 1,5 is used for variable loading. For permanent loading the safety ULS factor 0,9 has been applied, seeing that this load has a positive effect on the stability. First, the minimal amount of ballast is considered, namely 0,6 kN/m^2. This value is specified as the minimal value by building codes to guarantee that the roof covering does not come loose from the roof. Then, a ballast load which is twice as heavy is investigated to see how this influences the stability.

The horizontal displacement of the interlocking glass column can be seen in Figure 7.2, as well as the vertical reaction forces. In accordance with the expected behaviour (Figure 5.5), there are no tensile reaction forces, meaning the stability is safe guarded. The column with larger horizontal displacement requires heavier roof ballast, as can be seen by comparing the reaction forces in Figure 7.2a to 7.2b. Figure 7.2c shows which part of the structure has higher compressive stresses (green > yellow > orange).

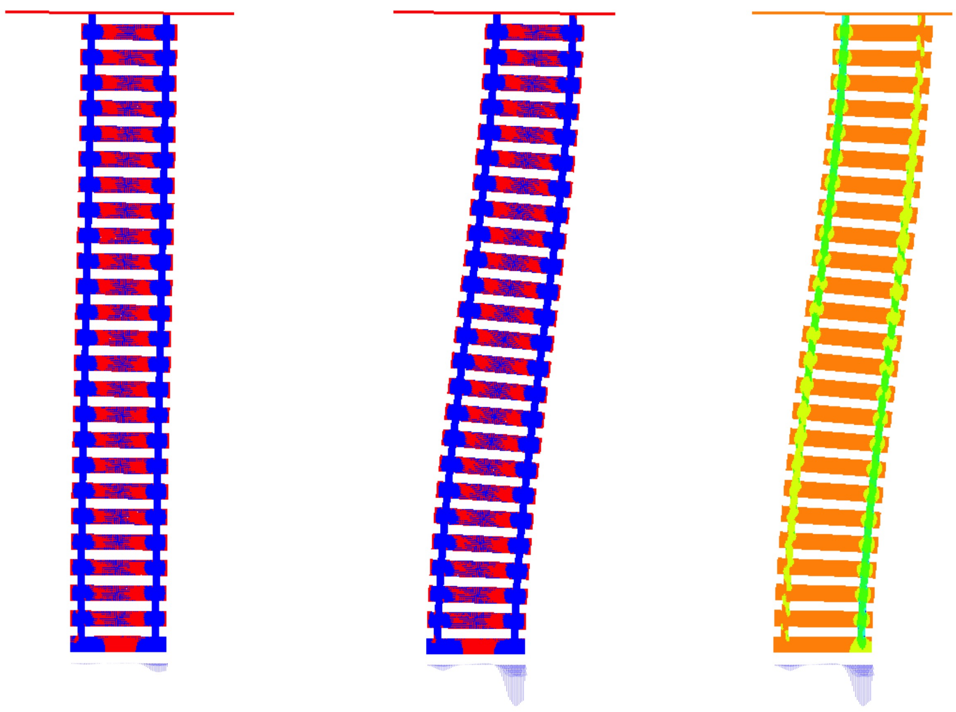

(a) (b) (c)

Figure 7.2: Image showing variant w=600 mm with ballast load 0,6 kN/m^2 & k_{spring} = 50000 N/mm **(a)**. In **(b)**: w=600 mm with 1,2 kN/m^2 ballast & k_{spring} = 5600 N/mm. Also, the reaction forces are shown at the base of the columns. Blue indicated compressive stresses and red tensile or neutral stresses. A discrete colour scale can be seen in **(c)**.

Figure 7.3 shows a force displacement diagram for two different component widths and ballast loads. The permissible amount of horizontal loading and horizontal displacement of the column is displayed, before instability occurs for load case 1. When instability occurs it is expected that the displacements go to infinity. However, this is very difficult to model, especially for loose elements. When the analysis is unable to converge for a variety of settings, it is assumed that instability occurs; the behaviour of the structure is modelled right up until instability occurs. This is then confirmed by checking the vertical reaction forces at the base of the column as previously explained. The graph is linear because the displacements are linearly related the the stiffness of k_{spring}. The minimally required values for k_{spring} have been used, which are summarised in Table 7.1. The allowable horizontal displacement of the column when 0,6 kN/m^2 ballast is applied, is very small. It is assumed that production tolerances will likely exceed these values. Therefore a ballast load of 1,2 kN/m^2 is preferred for this case study.

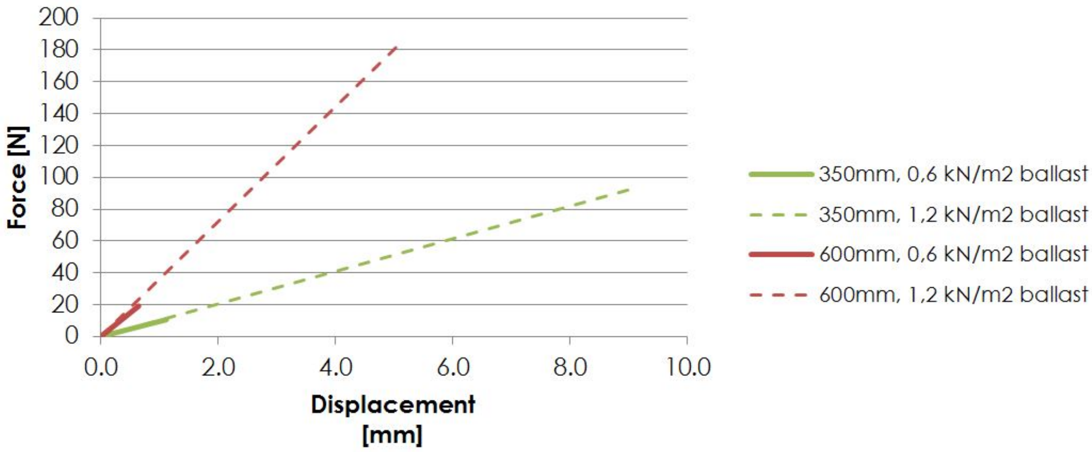

Figure 7.3: F,u diagram for when the column is stable for various parameters for LC1. This minimum value for k_{spring} is used.

The graph in Figure 7.4 shows the minimum value of k_{spring} required for the structure to remain stable. This is done for different width elements and two different ballast loads. The minimum and maximum values from the graph are summarised in Table 7.1. As can be seen, wider elements need a stiffer value for k_{spring}; this is because wider elements lead to a stiffer column which attracts more horizontal loading, resulting in larger displacement. A stiffer spring is therefore needed to limit displacement and stabilise the column. An increased ballast load results in k_{spring} needing to be less stiff. This is as expected and has been previously explained in Figure 5.5. The required k_{spring} is drastically reduced. Values for k_{spring} for 0,6 kN/m^2 were investigated with an increment of 1000 N/mm, while the 1,2 kN/m^2 with an increment of 100 N/mm. Both have been fitted with a linear trend line. Deciding on a ballast load with corresponding k_{spring} is partly a design choice. It is a trade-off between weight and stiffness. A stiff connection for the façade panels might be more difficult to assemble, while adding extra roof ballast might be more time consuming and requires extra resources. For this case study the ballast load of 1,2 kN/m^2 drastically reduces the required façade stiffness, when comparing it to the minimal required value. This heavier ballast load is therefore desired.

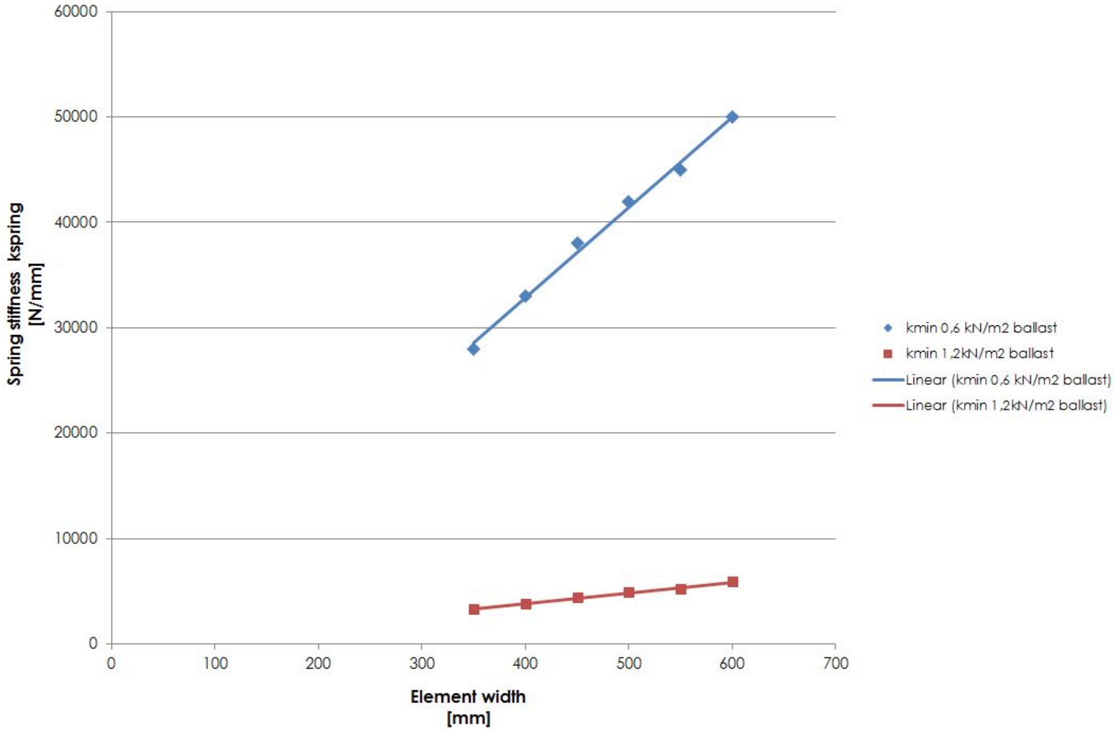

Figure 7.4: Graph showing the minimum required stiffness k_{spring} for different width elements and ballast load of 0,6kN/m^2 and 1,2 kN/m^2 for LC1.

Table 7.1: Minimal required k_{spring} value to guarantee stability

			k_{min} [N/mm]
LC1	w=350 mm	ballast=0,6 kN/m^2	28000
		ballast=1,2 kN/m^2	3300
	w=600 mm	ballast=0,6 kN/m^2	50000
		ballast=1,2 kN/m^2	5900

Loading combination 2 is similar to LC1, but is not governing for the stability. LC3 is not relevant for stability because it is symmetric downward loading with no horizontal loading.

7.3 Force distribution

The previous part has proven that the structure and column can remain stable under the relevant loading conditions, using realistic structural values for the following parameters: element sizes, façade stiffness, ballast loads and interlayer thickness. Next, the force distribution between the column and other structural elements will be determined. This way it can be assessed to what degree this new type of column contributes to taking up the applied forces. Both the horizontal and vertical force distribution will be investigated.

7.3.1 Horizontal force distribution

Table 7.2 is an overview of how much the column contributes to taking up horizontal loading for LC1. The percentage refers to the amount of load in reference to the total applied horizontal load. Though increasing the ballast load and width of the element both do increase the amount of horizontal load the column takes up, this is not a significant part of the total horizontal load. For all parameters the horizontal contribution of the glass column is less than 1% of the total applied horizontal load. The horizontal load is still mostly taken up by the façade fins and longitudinal façade panes (schematicised as k_{spring}).

Table 7.2: Reaction forces column for different width and ballast parameters

			$F_{h,reaction}$ [N]	%
LC1	w=350 mm	ballast=0,6 kN/m^2	10,6	0,02
		ballast=1,2 kN/m^2	92,6	0,16
	w=600 mm	ballast=0,6 kN/m^2	19,2	0,03
		ballast=1,2 kN/m^2	182,7	0,31

Next an element with a height of 200mm is investigated, which is twice the height of the above mentioned elements. Other assigned properties can be found in Table 7.3. The glass column takes up more load than 100 mm high elements, however again the amount of loading it takes up is insignificant when considering the total applied load. Increasing the height of the element presumable increased the stiffness of the column as a whole, however this increase is mostly attributed to using less interlayers.

Table 7.3: Horizontal load distribution for column with components with h=200 mm instead of 100 mm.

					$F_{h,reaction}$	%
LC1	w=350 mm	h=200 mm	1,2 kN/m^2	k_{min}=2800 N/mm	133,5	0,25

7.3.2 Vertical force distribution

To investigate how much the glass column contributes to taking up vertical loading, loading combination 3 (LC3) is investigated because it results in the largest compressive loading of the column. When considering downward symmetrical loading, it is expected that accounting for geometric nonlinearities is not necessary. The deformations are not so large that they alter the orientation of forces. The interfaces only present physical nonlinear behaviour under tensile loading.

Table 7.4 gives an overview of the vertical load distribution according to different analysis methods. The sum of vertical reaction forces at the base of the column is the same for the following analysis types: linear analysis, geometric linear analysis and Total Lagrange geometric nonlinear method. The Updated Lagrange geometric nonlinear method sticks out and is different. Also, the S_{yy} stresses are roughly ten times larger for this analysis type than for the other analyses. This seems odd, especially because the reaction forces are smaller. This, in combination with above reasoning leads to the conclusion that these results are invalid; this analysis method does not seem fit for this specific loading combination.

Table 7.4: Vertical load distribution for LC3 according to different type of analysis. The Updated Lagrange method is considered invalid for this specific loading combination.

	Linear		Geometric linear		Total Lagrange		Updated Lagrange	
	$F_{res,vert}$ [N]	%	$F_{res,vert}$ [N]	%	$F_{res,vert}$ [N]	%	$F_{res,vert}$ [N]	%
LC3	22935,8	15,1	22881,3	15,1	22885,6	15,1	8937,2	5,9

In Table 7.5 the influence that the height variation has on the vertical force distribution is shown. A geometric linear analysis was conducted, because it was concluded that this is a valid analysis procedure for this load case. A higher element significantly increases the amount of load taken up by the column. This is because the amount of interlayers is reduced, which increases the overall stiffness of the column. Note that the notch depth of the interlock remains constant, namely 10 mm. This, in combination with the slightly different self-weight of each column, results in the percentage not being exactly twice as much. The element with a width of 350 mm and a height of 200 mm stays within the design limitation (mentioned in Section 8.4.4) of weighing less than 8 kg per component. Furthermore, wider elements do not necessarily contribute to taking up more vertical load.

Table 7.5: The difference in vertical reaction forces for different height components.

			$F_{res,vert}$ [N]	%
LC3	w=350 mm	h=100 mm	22091,4	14,8
		h=200 mm	34333,8	23,0

In order to investigate whether the demountable column is able to take up a more significant amount of the vertical load, the interlayer thickness is reduced from 4mm to 1mm. This is done by adjusting the value in Formula 6.1. The result can be seen in Table 7.6. The difference between the column made from h=100 mm and h=200 mm components is less large than the results in Table 7.4. The difference between a 4 mm and 1 mm thick interlayer is smaller for the h=200 mm components, because this configuration uses less interlayers than a column made of h=100 mm components.

Table 7.6: The reaction forces for when the interlayer thickness is reduced to 1 mm instead of 4 mm.

				$F_{res,vert}$ [N]	%
LC3	w=350 mm	k_n=137 N/mm^3	h=100 mm	49193,0	32,9
			h=200 mm	57966,7	38,7

The glass column as proposed in this research contributes with to the vertical force distribution by taking up a maximum of 39 % of the vertical loading. This is when elements are 200 mm high and the interlayer has a thickness of 1mm. The soft interlayers reduce to overall stiffness of the column, resulting in it to take up less load than a traditional, solid column.

7.4 Stress distribution

Finally, the stress distribution is investigated to gain understanding of the location of peak stresses and to check whether they are permissible. Especially local tensile stresses are of interest because glass is susceptible to cracking under tensile loading. A maximum allowable tensile stress of 6,53 MPa is allowable, as explained in Appendix A.

Loading combination 1 is governing for tensile stresses, especially when minimal roof ballast is applied. Figure 7.2c shows the stresses for the entire column for loading combination 1. It is clear how the load is transferred through the column by means of compression. Also the parts with minimal compression can be seen. The tensile stress concentrations stay within the allowable limits for all loading combinations. Figure 7.5 shows the stresses in more detail. The S_{yy} stresses are governing over the S_{xx}. The tensile stresses in Figure 7.5b can be seen; some are located where the curved interlock is. According to the numerical analysis, the values are within allowable limits. Future physical testing can be used to confirm this. When applying heavier roof ballast, the tensile stresses further decrease. However, this second option is contradictory to the demountable concept; using as little material as possible is desirable. Also, increasing the ballast leads to a higher overall self-weight, with larger forces and stresses as a result. Therefore applying more than twice the minimal amount of ballast load is not investigated in this research.

(a)

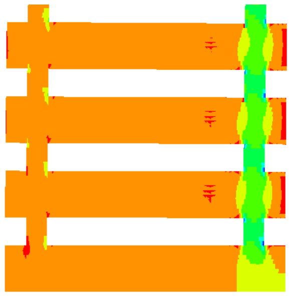

(b)

Figure 7.5: The locations of (tensile) stress concentrations can be seen for S_{xx} **(a)** and S_{yy} **(b)** for LC1. Note that the colour scale is different for both images. A roof ballast load of 0,6 kN/m^2 has been used.

Because the column does not take up a significant amount of horizontal loads, the S_{xx} stresses are very small. Tensile S_{yy} stresses stay below the allowable value of 6,53 MPa for asymmetric wind loading conditions (LC1 and LC2) and decrease when roof ballast load is increased. Symmetric compressive loading from loading combination 3 does not result in significant tensile peak stresses. More investigation on stress concentrations is therefore not deemed necessary for this research.

7.5 Outcome parameter study

There are many combinations of parameters that lead to a feasible column design. Two recommendations of feasible designs are given, based on the following aspects:

- A significant horizontal displacement of the column is possible before instability occurs. This way manufacturing tolerances have a smaller effect on the stability.
- The amount roof ballast fits with the design concept of a temporary building; for this design that is a maximum of 1,2 kN/m^2, which is twice the minimum value defined in building codes.
- The component dimensions are aesthetically pleasing and are in proportion with the column and overall design.

Table 7.7 and 7.8 show two examples of chosen parameter combinations for a feasible column design according to the previously investigated aspects: stability, force distribution and stress concentrations. Both examples do not take up significant horizontal load; therefore this is not included in the tables. The stress concentrations are within the allowable limits for both examples.

Table 7.7: Example 1 of a combination of parameters that lead to a feasible design

Component dimensions	Width	350 mm
	Height	100 mm
Pavilion parameters	Ballast load	1,2 kN/m^2
	Minimal required facade stiffness	3300 N/mm
	Interlayer thickness	4 mm
Outcome	Stability (u_{max})	9,1 mm
	Vertical force distribution	15 %

Table 7.8: Example 2 of a combination of parameters that lead to a feasible design

Component dimensions	Width	350 mm
	Height	200 mm
Pavilion parameters	Ballast load	1,2 kN/m^2
	Minimal required facade stiffness	2800 N/mm
	Interlayer thickness	1 mm
Outcome	Stability (u_{max})	11,4 mm
	Vertical force distribution	39 %

IV Case Study

8 Design considerations 57
8.1 Introduction case study
8.2 Conceptual design
8.3 Loading conditions
8.4 Design choices & motivations

9 Final design 65
9.1 Introduction
9.2 Design
9.3 Demountable connections
9.4 Detailing
9.5 Assembly & demounting

8. Design considerations

8.1 Introduction case study

A case study is introduced to give context to this new type of interlocking, laminated glass column. The case study is a single storey, travelling pavilion in the Netherlands with a floor space of 10 by 10 meters. Pavilions are an ideal structure to test and display innovative materials and construction methods, because of their temporary nature and limited costs. The proposed pavilion can serve as a multi-purpose, open floor plan space and can be used for meetings, small exhibitions, or as extra workspace. Furthermore, it will serve as a state-of-art demonstration of the structural and architectural possibilities of this proposed concept of a column made of interlocking, laminated glass elements. It can be assembled and demounted multiple times and can stand in a variety of urban or rural settings.

8.2 Conceptual design

Interlocking glass components will form a column on which a timber 'Japanese' style roof is placed. The rhythm of the receding timber roof recurs at the base of the pavilion in the form of timber wrap-around bleachers, which is visualised in Figure 8.1. The pavilion is demountable and is made up of smaller elements that can be easily transported. The rhythm of alternating glass and open voids makes for an interesting visual image that is counter intuitive for a load bearing structural element. Transparency, reflection and refraction influence how the user perceives both the column and the surrounding space.

Dry stacked elements fits with the concept of a temporary building. A large cross section is effective against buckling but also ensures the column is stable during assembly and needs little to no temporary supporting system.

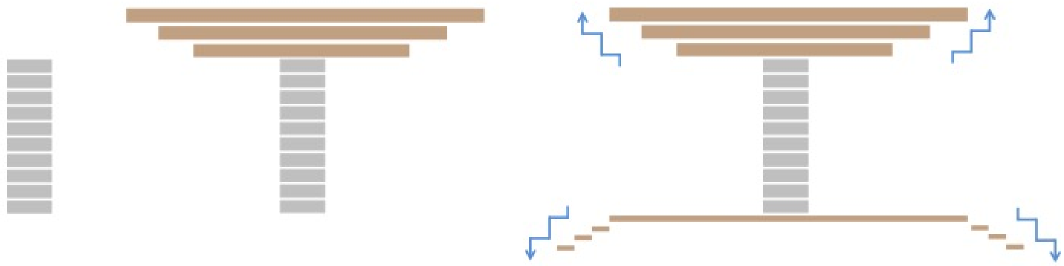

Figure 8.1: Concept visualisation

8.3 Loading conditions

The design will be loaded according to the Eurocode with wind, snow and variable loading. Because the pavilion will travel through the Netherlands, the least favourable wind load will be taken into account. For more detailed information on governing loads and load combinations see Appendix D.

One of the conditions for the column and structure to function properly is to prevent roof uplifting. In order to fit within the demountable concept, ballast will be used instead of increasing the self-weight of the roof structure. Locally acquired materials will be used such as: gravel, stones or tiles. This also reduces transportation. Uplifting in both the column and façade are undesired. The column and roof are not mechanically connected so in order for the roof to stay in place it needs to be sufficiently heavy. However also tensile loading in the stabilising façade is not desirable. First of all, because glass has limited tensile capacity and secondly, uplifting would require extra heavy foundations and special attention to detail.

8.4 Design choices & motivations

Many different design aspects have been considered before coming to the design presented in Chapter 9. Here this design process will be explained and trade-offs will be visualised.

8.4.1 Material choice

A glass column is an interesting balance between transparency and light reflection. Most of all, glass is a very strong material with a high compressive strength. In order to make the column demountable, it will be made up of smaller handle-able elements that can be stacked on top of each other. Laminated glass has extra incorporated redundancy and is quicker to produce than cast glass. Furthermore, lamination guarantees consistently high quality. Annealed glass has been chosen because it is most economical and sufficiently strong for this specific application. Timber has been selected on the basis of aesthetic reasons. Furthermore, timber is a renewable material and a widely applied material for temporary structures.

8.4.2 Load transfer column

There are three main design solutions for the load transfer of this modular glass column (Figure 8.2). Of course a hybrid version, incorporating multiple of these design solutions is also possible. These three strategies will be explained below, after which a trade-off between these solutions is made in Table 8.1.

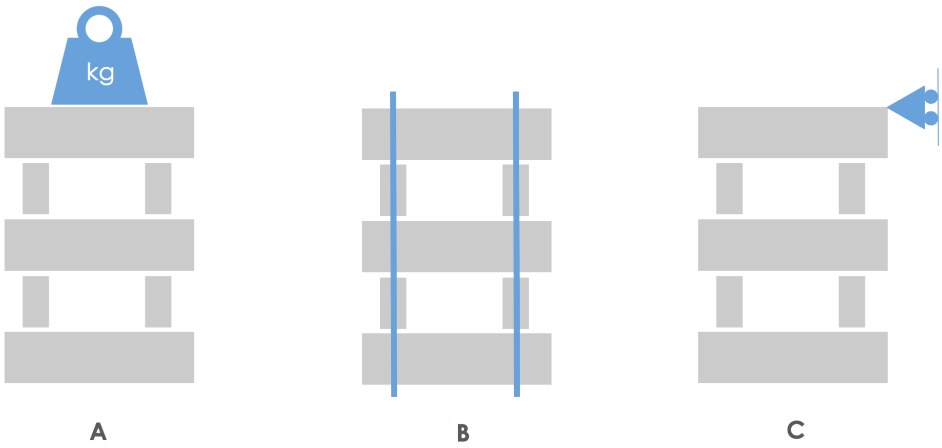

Figure 8.2: Schematic image of the different possible load transferring systems for the glass column.

Design solution A
The self-weight of the roof is large enough to counteract the wind induced uplifting. This way the column does not need to take up axial tensile forces. The roof beams are connected together (mechanically or interlocking) to prevent them from blowing away. Alternatively ballast can be placed on the roof instead of increasing the self-weight.

Design solution B
The structure is held together by vertical tensile elements, similar to the Optical House described in Section 2.3.1. These take up tensile forces, while the glass components take up compression. The drawback of this solution is that these tensile bars would be visible through the glass elements. The bars or cables can be used with or without post-tensioning. Post-tensioning would increase tensile capacity of the column because the induced compression would need to be overcome first. On the other hand, the compressive capacity would be reduced.

Design solution C
A secondary structure aside from the column can help take up (tensile) forces and will allow for structural redundancy. This method will also limit displacements. A variety of possibilities can be applied, which can be seen in Figure 8.3.

Table 8.1: Trade-off matrix global load transfer system

	Design A	**Design B**	**Design C**
Minimal visual impact	++	-	+
Efficient use of material	- -	+	+-
Redundancy	-	-	+-
Assembly ease	+	-	+
Ability to take up tensile loading	+	+	+
Ability to take up bending moment	- -	-	+-
Total	**+-**	**-**	**+**

A trade-off between the different design solutions can be seen in Table 8.1. The assessing criteria fit case study and the conceptual idea of a demountable structure; Design C is deemed most suitable and will be further elaborated on. The other design solutions will be disregarded from this point onwards.

8.4.3 Load transfer pavilion

The different potential load transferring solutions for the pavilion are depicted in Figure 8.3. The variants are discussed and compared below.

Design solution C1

This design solution makes use of extra columns made from a more traditional building material such as timber. The columns would need to be able to take up bending moment in order to transfer part of the applied horizontal load.

Design solution C2

Structural glass panels can take up horizontal wind loading by functioning like wind bracings usually do. At the same time, these structural elements serve as a façade. The façade can be laterally supported with glass fins to ensure maximum transparency.

Design solution C3

This design variant uses vertical cables to prevent the roof uplifting caused by wind suction. The drawback of this solution is that these vertically oriented cables are unable to take up horizontal loading.

Design solution C4

These inclined cables can take up horizontal forces, reducing the horizontal reaction force (and thus the bending moment) in the glass column. The cables fit nicely with the concept of a temporary pavilion because they are easy to assemble and take up virtually no space. This solution however does not incorporate structural redundancy into the design.

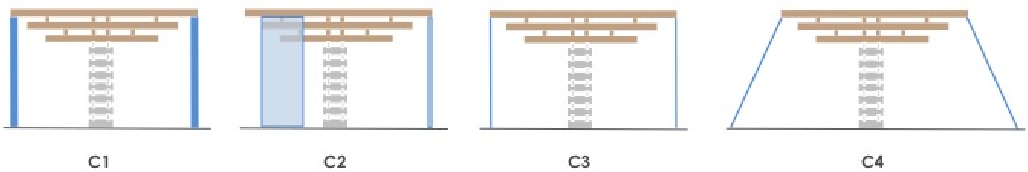

Figure 8.3: Schematic image of the different possible load transferring systems for the pavilion.

Table 8.2: Trade-off matrix for stabilising methods for the pavilion

	C1 Columns	C2 Structural glass panels	C3 Vertical cables	C4 Inclined cables
Minimal visual impact	-	++	++	+
Demountable concept	-	+-	++	++
Efficient use of material	-	+	++	++
Assembly ease	+	+	++	++
Structural redundancy	++	+	- -	- -
Compressive loading	+	+	- -	- -
Tensile loading	+	+	+	+
Bending	+	+	- -	+
Freedom end connections	++	++	- -	- -
Total	**-**	**++**	**-**	**+**

8.4.4 Element design

The elements should meet the following design criteria:

- Elements should be handle-able for builders during construction and therefore weigh less than 8 kg each.
- The elements should interlock in a logical and intuitive way so safe construction is insured.
- There should be as many identical components as possible so both production and construction are easy and fast.
- The shape of the interlock should be gradual and round in order to prevent (tensile) stress concentrations.
- The overall shape of the component should not be sensitive for parts damaging or breaking off.

There are different ways to fabricate the designed element. Laminated is desired over adhesives because it is quicker, cheaper and results in consistent high quality. The trade-off between the different production techniques can be seen in Table 8.3. It becomes clear that laminated float glass in combination with waterjet cutting is most favourable for this case study.

Table 8.3: Trade-off matrix for different production techniques to produce the glass components.

	Extruded	**Cast**	**Laminated float + waterjet cutting**
Form freedom	-	+	+
Minimal visual impact	+	+	-
Safety	+-	+-	++
Production ease	-	-	+
Production time	+	- -	+
Low costs	+-	-	+
Tolerances	-	+	+
Total	**-**	**+**	**++**

Now that lamination has been selected as production method, a few limitations of this technique are discussed and dealt with. Firstly, above a certain thickness, glass panels become much more expensive. For this case study the thickest economically available float glass is chosen, which is 15 mm thick. Secondly, lamination generally allows for no more than 5 layers being laminated together. Therefore each element will be made up of 3 x 15 mm as structural layers which will be be protected by a thin sacrificial layer of 2 - 4 mm on either side, as can be seen in Figure 8.4b and 9.8.

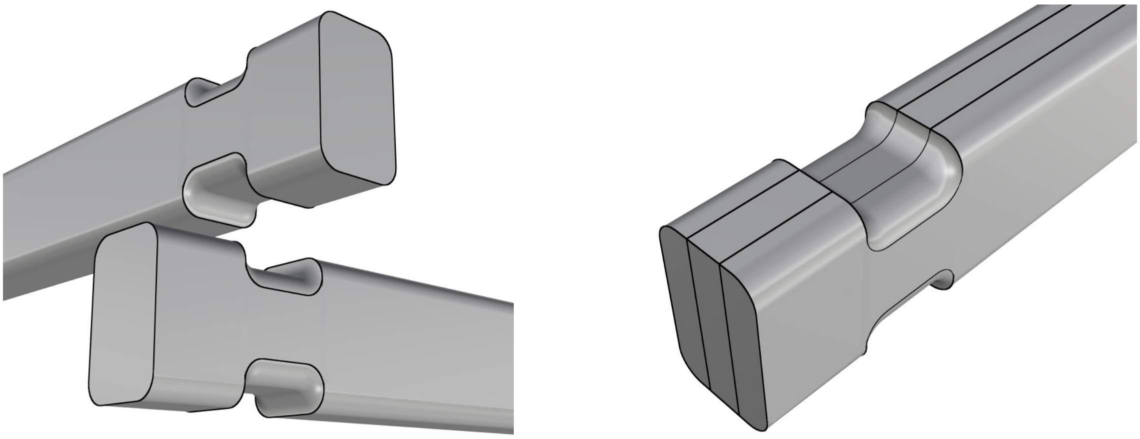

(a) (b)

Figure 8.4: The interlock of the elements can be seen in **(a)** and the different layers of laminated glass in **(b)**.

The interlock has been designed so elements can be assembled at a right angle. The assembly is intuitive and logical. The edges of the interlock are round to prevent stress concentrations.

8.4.5 Top & bottom connections

The glass façade fins follow designs that are common practice. For the bottom a steel shoe will protect the bottom from damage. Between the glass and steel will be a neoprene layer. The façade fins will be hinged connections.

For the glass column, the stacked concept will be followed as much as possible. The bottom of the glass column will be protected against damages. This way, cleaning with a mop or vacuum cleaner will not damage the bottom few elements.

8.4.6 Safety & redundancy

On the component level, the chance of damaged and breakage is drastically reduced by the sacrificial layer on either side. The column will unlikely be damaged on the inner side of the column. However, when considering easy and quick assembly, it is desired that components are symmetrical. This way no mistakes can be made during assembly and there is always a sacrificial layer to protect the components. Therefore the design choice has been made to apply a sacrificial layer on either side of the component, instead of only on one side.

Despite the sacrificial layers, damage is still possible (Figure 8.5); if the component is hit on either of its ends, at the edge curvature or on the top or bottom, damage is possible. However, these lastly mentioned options are unlikely due to the stacked configuration. Laminated glass retains sufficient bearing capacity in the case of cracks and damages, therefore it is deemed an acceptably low risk.

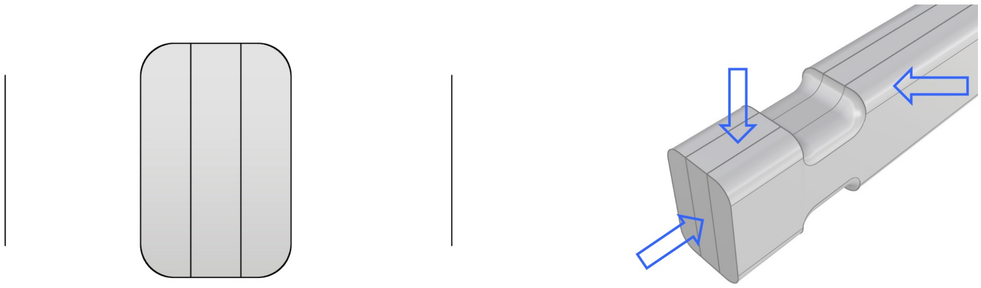

(a) (b)

Figure 8.5: The dimensions of the sacrificial layers in comparison to the element in **(a)**. Damage is possible in the areas pointed out in **(b)**; these are not protected by the sacrificial layers.

The demountable glass column retains sufficient load bearing capacity if damages. Furthermore, the pavilion as a whole has incorporated redundancy through the structural glass façade system. This is the alternative loading path aside from the glass column. Axial loading and lateral wind loading can be taken up.

8.4.7 Requirement assembly & demounting

Assembly and demounting should be logical. The glass column should not need to be supported during construction. All elements should have the dimensions to fit into a standard sized truck.

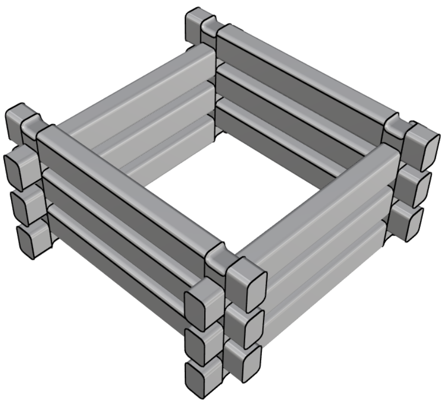

Figure 8.6: Stacked components

9. Final design

9.1 Introduction

This chapter shows drawings of the final design of the pavilion. Also fabrication, assembly and demounting will be discussed in more detail.

9.2 Design

Figure 9.1: Impression of the outside of the pavilion.

Figure 9.2: Impression drawing of the inside of the pavilion.

9.3 Demountable connections

Different demountable connections will be discussed in a conceptual manner. In Figure 9.3 is an overview of the different connections that will be considered.

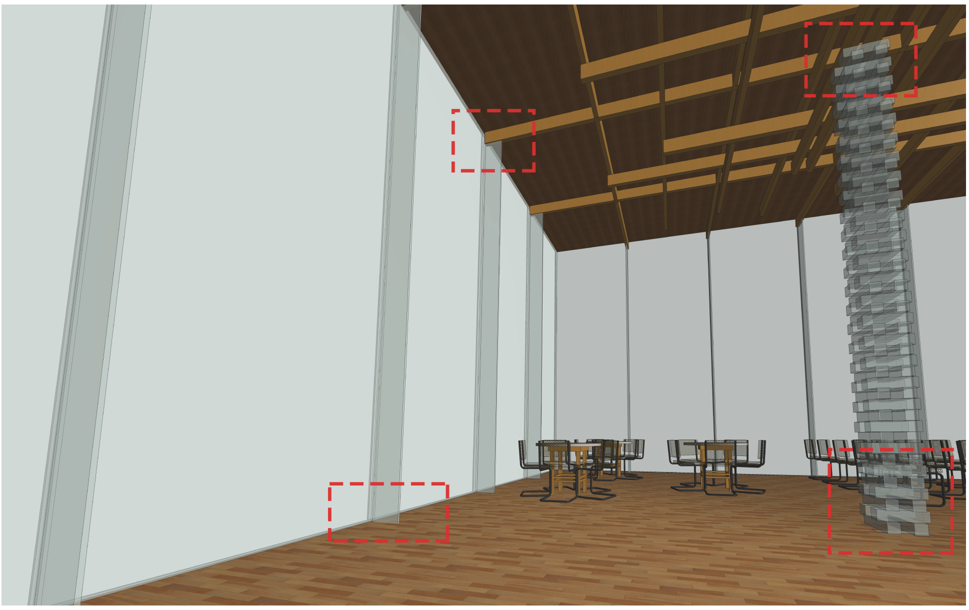

Figure 9.3: An overview of the different connections that will be covered.

9.3.1 Top connection glass column

The timber beams are stacked on the top glass components. The first timber beam stacked onto the glass column will be fitted with the same rounded interlock as displayed in Figure 8.4a. The other timber beams can be fit with straight interlocks, or be bolted together.

9.3.2 Bottom connection glass column

Figure 9.4 shows a sketch of what the bottom connection of the glass column could look like. Interlocking timber components surround the bottom glass components. This way, the base of the glass column is protected from damages. The stacked timber fits with the design of the rest of the pavilion. The laminated glass base component can be flat at the bottom. A neoprene layer is between the bottom glass component and surface below.

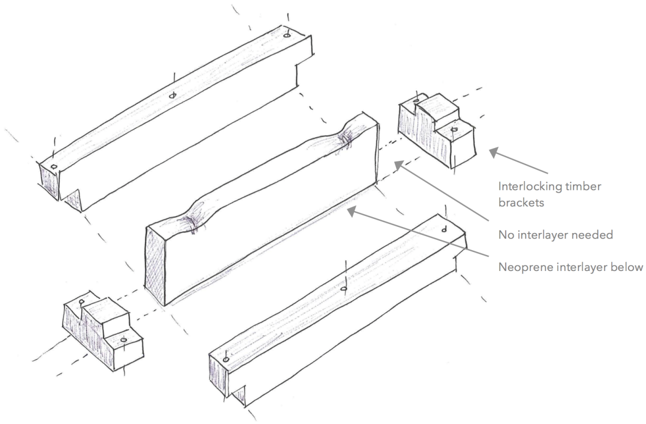

Figure 9.4: A sketch of what the bottom connection of the glass column could look like.

9.3.3 Top connection roof-façade fin

Figure 9.5 shows how the timber roof beam and glass fin meet. The connection is detailed to be a hinge. The slit in the timber beam allows for some adjusting if needed. After the glass fin is produced, a hole is drilled into the glass. Then the edges of the hole are polished to prevent cracks from propagating from there.

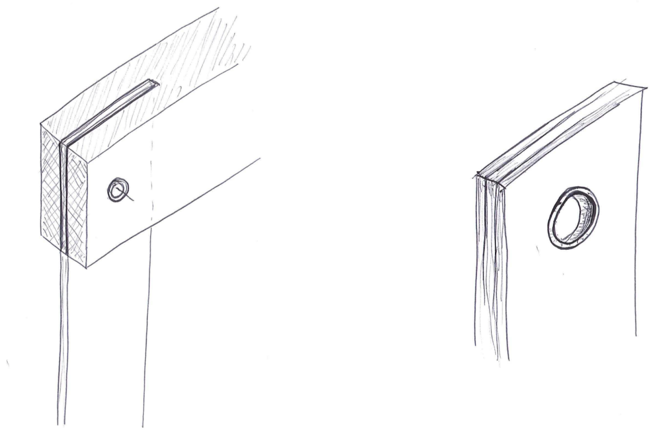

(a) (b)

Figure 9.5: Drawing of detail top glass façade fin. **The roof-facade connection can be seen in (a)** where the timber beam and glass facade fin connect. The glass plate can be seen in **(b).**

9.3.4 Bottom connection façade fin

This type of connection can be found in many existing buildings. It is important that the bottom 10 cm of glass is protected to prevent damages. Figure 9.6 shows an example of a usable bottom connection for the façade fin. More transparent connections are possible, however this one has the desired protection at the bottom. Also, bolting the metal shoe to the foundation fits with the demountable concept.

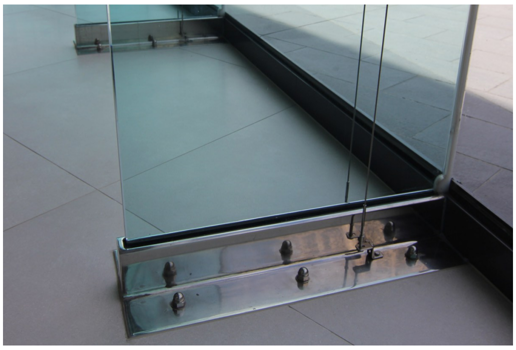

Figure 9.6: An example of a bottom connection detail for a façade fin, retrieved from GJames (2013).

9.4 Detailing

9.4.1 Components

Figure 9.7 shows detailed images of the interlock. The curvature can be seen, along with the different structural glass layers.

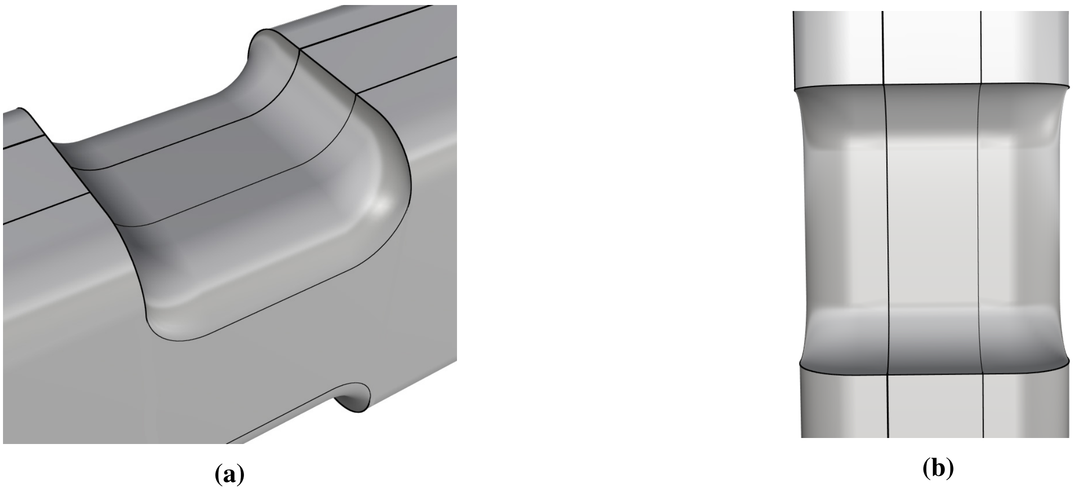

Figure 9.7: A detail of the interlock in **(a)**. The flat and curved parts of the interlock can clearly be seen in **(b)**.

9.4.2 Component manufacturing

To fabricate the proposed laminated glass components, the following steps will be taken:

- Step 1: The glass plates are watjet cut into the desired shape using a 3D waterjet cutter. For the middle structural glass plate and the sacraficial layers, a 2D waterjet cutter suffices to produce the geometry. An exploded view with 3 structural layers of glass and 2 sacraficial layers on either end can be seen in Figure 9.8. As can be seen, the outer structural glass layers are most challenging to fabricate because of the curvature.
- Step 2: PVB interlayers are placed between the glass plates and they are laminated together in an autoclave.

- Step 3: When using water jet cutting as production method, post-processing generally is not necessary because the edge damages are much less significant than when using traditional cutting. The interlock is the most important part of the geometry. If necessary, the edges can be smoothed by hand to prevent peak stress concentrations. The interlayer will make up for slight irregularities in the interlock caused by production.

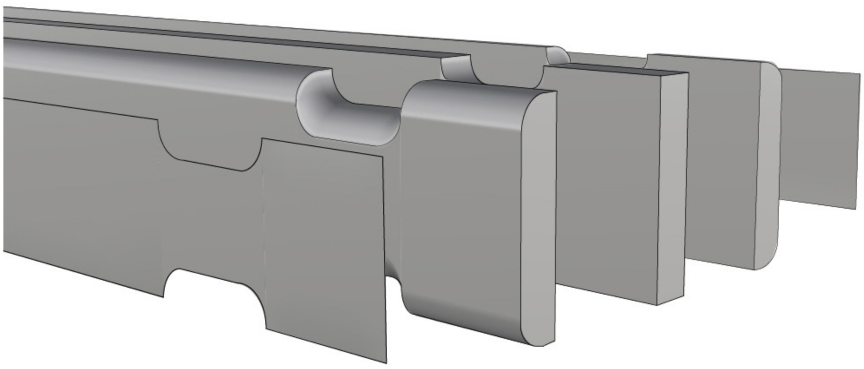

Figure 9.8: An exploded view of the three structural layers and the two sacrificial layers.

The manufacturing challenge lies with the relatively narrow interlock mechanism, making it difficult to reach for certain machinery. The schematic image in Figure 9.9 shows possible imperfections after manufacturing. The left image show the idealised and desired interlock geometry; the middle image displays small surface flaws due to the waterjet cutting. The right image displays slight differences in vertical position of the separate structural glass plates. These defects will likely be small, because of the accuracy of water jet cutting. Figure 9.9 also displays the interlayer, which can accommodate for some of the surface defects as well.

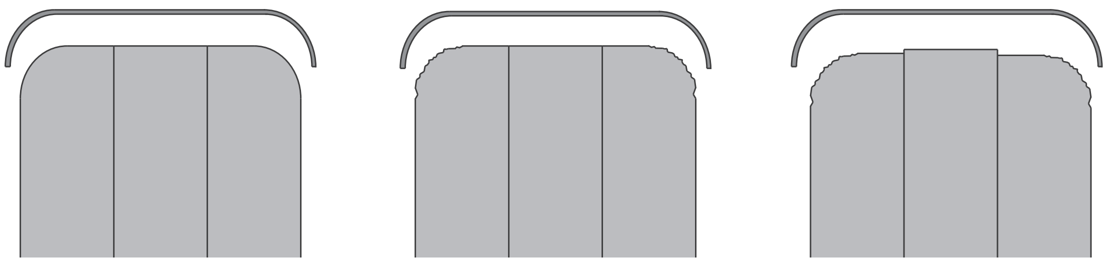

Figure 9.9: The cross section of the interlock of the geometry. Three differently finished en results are shown in a schematic drawing.

9.5 Assembly & demounting

Figure 9.10 shows the step by step assembly sequence of the pavilion. Demounting happens the same but in opposite order.

- Step 1: The wooden platform will be built up. It is assumed the the foundation is strong enough to support the pavilion.

- Step 2: The laminated glass components will be stacked to form the column.
- Step 3: The glass façade and the glass façade fins are assembled. Construction will start in the corner to ensure lateral stability. The façade fins also guarantee lateral stability for the façade. Temporary supports should be prevented if possible.
- Step 4: The remaining façade elements and fins will be assembled.
- Step 5: Temporary supports will most likely need to support the glass column, in order to prevent it from falling over when the roof is aligned with the column. The timber roof beams will be connected to the glass façade fins. There are two options. Either the roof can be completely assembled on the ground and then hoisted into place. The downside of this method is that all the roof beams, façade fins and glass column need to be aligned at once. The other option is to assemble the roof beam by beam. This makes it easier to line up the connections. Roof ballast will be added immediately.
- Step 6: The finishing touches will be done. The doors will be added and furniture will be put inside.

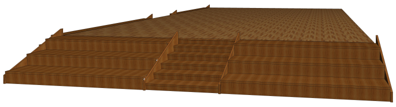

(a) Step 1

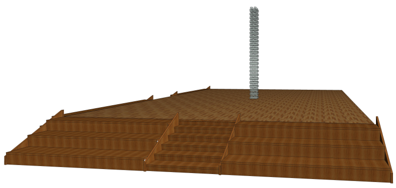

(b) Step 2

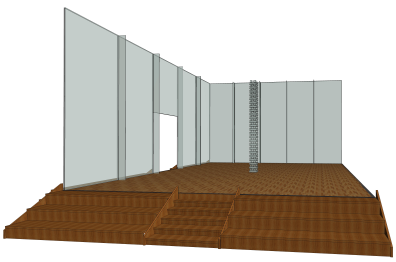

(c) Step 3

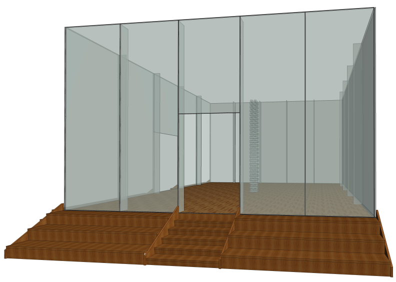

(d) Step 4

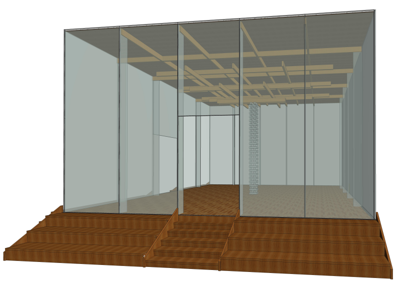

(e) Step 5

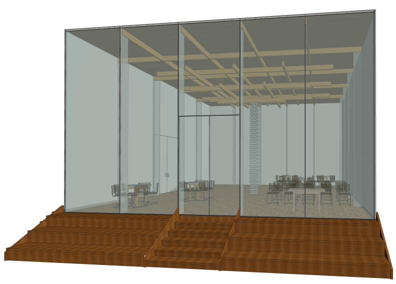

(f) Step 6

Figure 9.10: The assembly order of the pavilion is displayed.

V

Conclusions & Recommendations

10	**Conclusions**	**75**
10.1	Conclusions column in case study context	
10.2	Conclusions column	
11	**Recommendations**	**79**
	Bibliography	**83**

10. Conclusions

10.1 Conclusions column in case study context

The aim of this research has been to provide a feasible design for a novel type of glass column, namely a demountable, interlocking column made of laminated glass components. This has been done by investigating various structural parameters, as well as design aspects. The proposed case study of a travelling pavilion gives the glass column context and realistic boundary conditions. After careful and extensive consideration, recommendations are made for a variety of structural parameters and design aspects in order to achieve a functioning, feasible column design.

10.1.1 Structural functioning

A Finite Element Analysis (FEA) has been used to investigate the following: stability, force distribution and stress concentrations of a column in the context of a case study of a demountable, travelling pavilion. This has been done for the following parameters: component dimensions, roof ballast, façade stiffness and interlayer thickness. There is an absence of research and results on this specific type of glass column, therefore literature has been consulted on glass material properties in general and similar glass columns and structures. The input of the numerical analysis has been carefully considered and motivated; analytical predictions served as a reference check for the FEA output. The outcome of this FEA has therefore been judged as valid for this design study, and was used to iterate and adapt the column design. Finally, a combination of parameters have been recommended that lead to a feasible design (Section 7.5).

The proposed interlocking column is deemed to be stable when there are no tensile reaction forces at the base of the column. Depending on the chosen parameters, the column is able to horizontally displace between 0,6 mm and 9,1 mm before instability occurs. Using a ballast of 1,2 kN/m^2, instead of the minimal value of 0,6 kN/m^2, greatly increases the column stability, while the added load is acceptable in terms of compressive stresses and demount-ability. This heavier roof ballast load is therefore desired.

The demountable column made of laminated glass components as defined in this research is unable to take up significant horizontal loading for the investigated parameters. The proposed column therefore does not contribute to stabilising the structure. Though increasing the width of the column components does increase its ability to take up horizontal loading, this is not a significant amount compared to the total applied horizontal load on the case study. For a variety of parameters, the column as previously defined takes up less than 1 % of the total horizontal load. Most of the load is transferred to the foundations by the façade fins and façade panels longitudinally oriented to the horizontal load direction.

Depending on the chosen parameters, the proposed column is able to take up between 15 % and 39 % of the vertical loading under the case study loading conditions. The maximum percentage of 39 % is achieved when the least amount of interlayers as possible are used by making the glass components as high as possible. For this configuration, components are 200 mm high and the interlayers 1 mm thick.

The tensile stress concentrations proved to stay below the allowable value of 6,53 MPa. There are permissible tensile stress concentrations located at the interlock mechanism, where minor fabrication defects will be. Tensile peak stresses are largest at the base and top of the column, where the least compression is.

10.1.2 Design aspects

An extensive amount of design aspects have been discussed. A variety of design solutions were traded off against one another based on: structural functioning; safety; material and fabrication limitations; aesthetics and fitting the demountable concept. These carefully considered trade-offs have been visualised and have resulted in design choices and fabrication suggestions.

The economically attractive, annealed float glass proved strong enough to use for the proposed interlocking laminated components for the glass column. Each component is made of 3 x 15 mm thick structural layers and is protected on either side by means of a sacrificial layer. The interlock is gradual and the rounded shape prevents tensile peak stresses. To fabricate the components, it is proposed to 3D water jet cut the glass plates before laminating them together. The risk of damage has been minimised. Moreover, the glass column has sufficient redundancy because the laminated components retain sufficient bearing capacity in case of damage. Also, the structural glass façade serves as secondary loading path in the case of severe damage.

Though the top and bottom connections of the stacked glass column have not been detailed as pure hinges, the column is able to take up the corresponding forces. This is a great advantage because it is not necessary to carefully detail the connection to be a pure hinge.

10.2 Conclusions column

The interlocking method in combination with self-weight and ballast does not allow for significant horizontal load to be taken up by the column. Such a column does not contribute to stabilising a structure. Absence of the ability to take up tension is the greatest limiting factor.

The soft interlayers are the limiting aspect of such an interlocking glass column. This greatly reduces the overal stiffness of the column, reducing the amount of vertical load the column takes up. Limiting the amount of interlayers and increasing the interlayer stiffness is favourable and allows for the column to take up a larger portion of the total load.

For this research the stresses stayed within allowable limits. However, when such an interlocking column takes up a larger amount of load, tensile stresses could become a more crucial part of the design checks.

Glass columns may currently only be applied in single storey buildings because of fire regulations. This is the largest limitations; the strength of the column does allow for the application of larger loads.

11. Recommendations

- For further research it is proposed to investigate connections between the interlocking laminated glass components that are able to take up tension. The absence of mechanical connections between the components namely proved to be a significant limitation of the proposed column design under the specified loading conditions. Such a connection should meet the requirements of being demountable; using rope to tie the elements together is worth investigating. This method will lead to stress concentrations; tensile stresses should remain below the allowable tensile stress value.

- For this research, the chosen FE input parameters for the interlayers are based on a limited number of experimental tests that are presented in literature. More research on the behaviour of interlayers under compressive loading is necessary in order to obtain a larger amount of test results, increasing their reliability. Insights that can be achieved with physical testing, include but are not limited to: contact area between the glass-interlayer for laminated components, homogeneous interlayer thickness and interlayer stiffness. These test results can then be translated to values for numerical input, resulting in more reliable and inclusive input, and thus output, of Finite Element analyses in the future.

- It is recommended to conduct physical laboratory experiments to further verify the outcomes and conclusions of this research. Aside from verification, these physical experiments will provide additional insights, especially concerning the influence of fabrication and manufacturing defects on the column's strength and failure behaviour. Also, the minimal required interlayer thickness to limit tensile stresses for (3D) water jet cut, laminated components can be determined by using physical experiments. How future physical testing relates to the research conducted in this thesis can be seen in Figure 11.1.

- In order for the column to contribute more significantly to taking up loading, stiffer interlayers are desired. Increasing interlayer stiffness however, is conflicting with the desire to avoid stress concentrations of the glass geometry. This delicate trade-off needs to be confirmed with experimental testing. Various materials can be investigated to use as interlayers; the choice is not necessarily limited to examples from existing literature. Analytical and numerical analyses are idealised representations of reality and account for defects and imperfections by applying safety factors. However, experimental testing should confirm safe functioning of an interlocking column using stiffer interlayers.

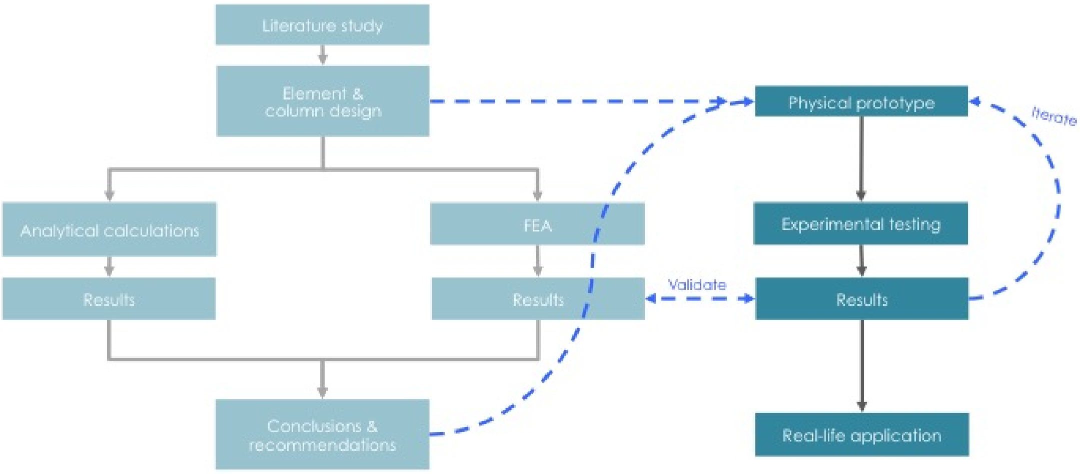

Figure 11.1: This research in relationship to possible future physical experimental testing.

- To limit the scope of this research, the buckling behaviour of this interlocking column was disregarded after analytical calculations showed instability would occur long before the buckling load was reached. However, this should be verified by either FEA or physical experiments. Furthermore, a suitable Finite Element software program should be selected for a buckling analysis. The software program Diana presented many problems and results proved unrealistic; the expertise at the university was insufficient to overcome these problems.

- Existing literature mentions the self-aligning ability of interlocking geometry as an advantage, especially under seismic loading. Whether or not this specific interlocking geometry, as defined in this design, presents this advantageous behaviour should be investigated. This can be done for both man induced earthquakes (like in Groningen) and tectonic earthquakes.

- The compressive strength of a glass column allows for large loads. This makes glass columns in general attractive to use for large, visually open floor plans such as lobbies of public buildings. However, building regulations prohibit the application of glass columns for buildings higher than one storey because of the poor fire resistance of glass. Fire resistance of laminated glass can be guaranteed and is common practice for glass separations. The fire resistance of a column made of laminated glass components, needs to be experimentally tested. When results are proven to reliable in terms of strength and redundancy, regulations regarding application of laminated glass columns could possibly be altered in the (far) future.

- In order to better fit within a sustainable and circular context, more research is needed to obtain high quality recycled laminated glass. This way the glass and plastic be re-used for new building purposes. Before recycled laminated glass can be used in real-life application for such a column, more experimental data is needed to verify the strength of this re-used material and in order to gain understanding on how the material strength is influenced by contamination with small amounts of remaining intermediary material.

Bibliography

Akerboom, R. (2016). *Glass columns, exploring the potential of free standing glass columns assembled from stacked cast elements* (MSc thesis). Retrieved from Repository TU Delft.

Aurik, M. (2017). *Structural Aspects of an Arched Glass Masonry Bridge* (MSc thesis). Retrieved from Repository TU Delft.

Aurik, M., Snijder, A., Noteboom, C., Nijsse, R., Louter, C. (2018). Experimental analysis on the glass-interlayer system in glass masonry arches. *Glass Structures & Engineering.*

Barou, L. (2016). *Transparent restoration* (MSc thesis). Retrieved from Repository TU Delft.

Bagger, A. (n.d.). Danfoss glass columns [Online image]. Retrieved from http://www.annebagger.dk/en/projects/glass-columns-at-danfoss.aspx

Breunese, A.J., & Maljaars, J. (2015). *Fire Safety Design.* Delft, the Netherlands: TU Delft.

Deloitte, (2016). *Economic study on recycling of building glass in Europe.* Retrieved from http://www.glassforeurope.com/images/cont/187_20647_file.pdf

Diana FEA, (n.d.). *DIANA-10.1 User's Manual – Analysis procedures.* Retrieved from https://dianafea.com/manuals/d101/Diana.html

Felekou, E. (2016). *Structural Glass in High-Rise buildings* (MSc thesis). Retrieved from Repository TU Delft.

GJames, (2013). Façade fin detail [Online image]. Retrieved from http://blog.gjames.com/glass-17/

Glass for Europe (2013). *Recycling of end-of-life building glass: Glass for Europe's contribution.*

Retrieved from http://www.glassforeurope.com/images/cont/187_987_file.pdf

Haldimann, M., Luible, A.,& Overend, M. (2008). *Structural Use of Glass.* Zürich, Switzerland: ETH Zurich.

Hammond, G.P. & Jones, C.I. (2008). Embodied energy and carbon in construction materials. *Energy, 161*(EN2), 87-98. Retrieved from http://opus.bath.ac.uk/12382/1/Hammond_%26_Jones_Embodied_energy_%26_carbon_Proc_ICE-Energy_2008_161%282%29_87-98.pdf

Hauk, C. (2015). Apple cube New York [Online image]. Retrieved from https://www.mactrast.com/2015/06/apple-fifth-avenue-store-to-be-renovated-will-move-to-temporary-fao-schwarz-location/

Heugten, R. (2013). *Load-bearing glass columns: the stacked column* (MSc thesis). Retrieved from Repository TU Eindhoven.

IQ Glass, (n.d.). Structural glass example [Online image]. Retrieved from https://news.iqglassuk.com/why-should-i-specify-low-iron-glass/

Jacobs, E.A.M. (2017). *Structural consolidation of historic monuments by interlocking cast glass components. A computational analysis of interlocking cast glass brickwork* (MSc thesis). Retrieved from Repository TU Delft.

Karmatrendz. (n.d.) Glass columns St-Germain-en-Laye [Online image]. Retrieved from https://karmatrendz.wordpress.com/2009/08/11/civic-center-in-st-germain-en-laye-by-atelier-9-portes-philippe-harden/#jp-carousel-9793

MVRDV, (2016). Crystal House [Online image]. Retrieved from https://www.mvrdv.nl/projects/crystal-houses

Lamination jumbo plate [Online image]. (n.d.). Retrieved from https://www.sedak.com/en/

Nieuwenhuijzen, E.J., Bos, F.P., & Veer, F.A. (2005). The Laminated Glass Column. *Glass Processing Days.*

Nijsse, R., & ten Brincke, E.H.J. (2014). Glass columns. *Challenging Glass 4 & COST Action TU0905 Final Conference.* London, United Kingdom: Taylor & Francis Group.

Oikonomooulou, F., Veer, F., Nijsse, R., & Baardolf, K. (2014). A completely transparent, adhesvily bonded soda-lime glass block masonary system. *Journal of Facade Design and Engineering.* DOI: 10.32333/FDE-150021

Oikonomopoulou, F., Bristogianni, T., Veer, F.A., & Nijsse, R. (2017). The construction of the Crystal Houses façade: challenges and innovations. *Glass Structures & Engineering.* DOI: 10.1007/s40940-017-0039-4

Oikonomopoulou, F., van den Broek, E.A.M., Bristogianni, T., Veer, F.A., & Nijsse, R. (2017). Design and experimental testing of the bundled glass column. *Glass Structures & Engineering.* DOI: 10.1007/s40940-017-0041-x

Oikonomopoulou, F., Bristogianni, T., Barou, L., Jacobs, E., Frigo, G., Veer, F.A., & Nijsse, R. (2018). A Novel, Demountable Structural Glass System Out of Dry-Assembly, Interlocking Cast Glass Components. *Challenging Glass 6 - Conference on Architectural and Structural Applications of Glass.* DOI: 10.7480/cgc.6

Omroep Venlo, (2015). Glass sphinx [Online image]. Retrieved from https://omroepvenlo.nl/nieuws/artikel/17590563

Optical house [Online image]. (n.d.). Retrieved from http://www.nakam.info/en/

Optical house construction [Online image]. (n.d). Retrieved from https://inhabitat.com/gorgeous-optical-glass-house-in-hiroshima-is-made-from-6000-glass-bricks/exif_jpeg_picture-12/

Petersen, R.I., Bagger, A., (2009). Structural use of glass: Cruciform columns and glass portals with bolted connections subjected to bending. *Glass Performance Days 2009.*

Schott (n.d.). Bridge TU Delft campus [Online image]. Retrieved from https://www.schott.com/innovation/en/technology-meets-aesthetics/

Sim, A. (2011). De Glazen Engel (by Herman Lamers) [Online image]. Retrieved from https://www.flickr.com/photos/akbar2/6314458385

Snijder, A.H., Veer, F.A., Louter, C., Nijsse, R. (2016). Modelling structural behaviour of a dry-assembled glass block bridge with soft PVC interlayer.

Snijder, A., Smits, J., Bristogianni, T. & Nijsse, R. (2016). Design and engineering of a dry assembled glass block pedestrian bridge. *Challenging Glass 5 - Conference on architectural and structural applications of glass.*

Sombroek, I. (2016). *Structural cast glass, a research process of design and experiment towards a feasible geometry for a cast glass element.* (MSc thesis). Retrieved from Repository TU Delft.

Soons, F.A.M., van Raaij, B.P.M., & Wagemans, L.A.G. (2014). *Quick Reference.* Delft, the Netherlands: Section Structural and Building Engineering.

The Danteum / Giuseppe Terragni [Online image]. (n.d). Retrieved from http://libguides.gwumc.edu/c.php?g=27779&p=170351

University of Washington. (n.d.). Eccentric loading; the Secant formula. Retrieved from http://faculty.washington.edu/nsniadec/ME354/W08/Lecture33_EcceBuck.pdf

University of Wellington. (n.d.). Embodied Energy Coefficients - Alphabetical. Retrieved from https://www.victoria.ac.nz/architecture/centres/cbpr/resources/pdfs/ee-coefficients.pdf

Veer, F.A., & Pastunink, J.R. (1999). Developing a Transparent Tubular Laminated Column. *Glass Processing Days.*

Veer, F.A., Van der Voorden, M., Rijgersberg, H., & Zuidema, J. (2001). Using Transparent Intumescent Coatings to Increase the Fire Resistance of Glass and Glass Laminates. *Glass Processing Days.*

Weller, B., Harth K., Tasche, S., & Unnewehr, S. (2009). *Glass in building: principles, applications, examples.* Regensburg, Germany: Aumuller Druck.

VI Appendices

A Design tensile strength glass 89

B Spring stiffness 91

C Other Diana considerations 93
C.1 Interface modelling considerations

D Loading conditions case study 95
D.1 Loading conditions
D.2 Governing loading combinations

E Load distribution: analytical prediction 99

F Case study design checks 103
F.1 Design checks glass fins
F.2 Design checks structural façade
F.3 Design checks timber roof

G Extra drawings pavilion 105

H Stress concentrations Diana 107

A. Design tensile strength glass

The following formula from NEN 2608:2014 can be used to calculate the design tensile strength of float glass:

$$f_{mt;u;d} = \frac{k_a \times k_e \times k_{mod} \times k_{sp} \times f_{g;k}}{\gamma_{m;A}} \tag{A.1}$$

The following values have been determined:

k_a	This factor accounts for the area of a glass plate. Because the area of each component is small, k_a = 1,0.
k_e	This value is related the edge quality of the glass. For glass that has not been heat treated or thermally strengthened, k_e = 0,8.
k_{mod}	This modification factor is dependant on the type of load, duration and exposure conditions. k_{mod} = 0,29.
k_{sp}	This factors relates to the area structure and depends on the fabrication method. For float glass k_{sp} = 1,0.
$f_{g;k}$	The characteristic bending strength of annealed glass is 45 MPa.
$\gamma_{m;A}$	The material factor is either 1,6 or 1,8. When wind loading is the governing variable load $\gamma_{m;A}$ = 1,6.

When filling these values in the following is attained:

$$\begin{aligned} f_{mt;u;d} &= \frac{1,0 \times 0,8 \times 0,29 \times 1,0 \times 45}{1,6} \\ &= \textbf{6,53} \quad \textbf{MPa} \end{aligned} \tag{A.2}$$

B. Spring stiffness

It is possible to determine k_{spring} by using the known relationship between the forces and displacements of the stabilising glass plates. Note that half of the distributed wind load goes straight the foundation as can be seen in Figure B.1.

$$k_{spring} = \frac{F_{wind}}{u_{horiz}} \tag{B.1}$$

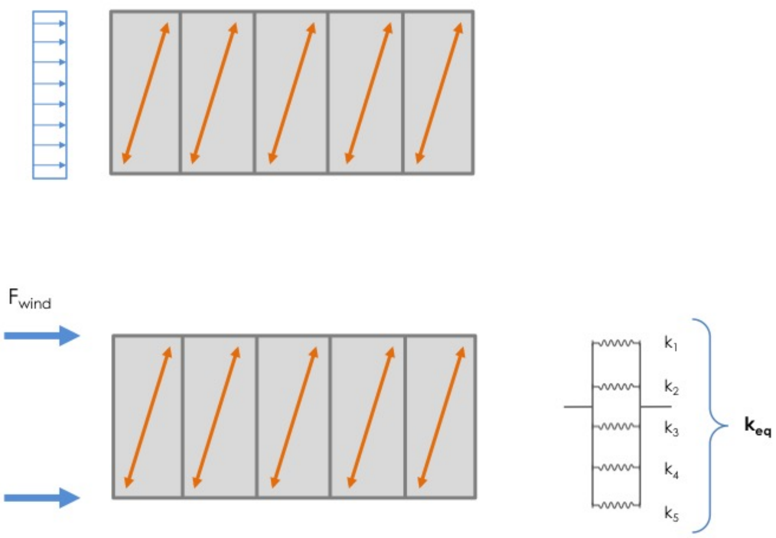

Figure B.1: Schematic image of façade taking up wind load through tension diagonals. This can be simplified as a spring.

First the strain in diagonal direction is computed, after which the strain in x-direction is determined.

Then the displacement in horizontal direction can be deducted.

$$\Delta l_{diagonal} = \varepsilon \cdot l_{diagonal} = \frac{N_{diagonal}}{EA_{required}} l_{diagonal} \tag{B.2}$$

$$with \qquad A_{required} = \frac{N_{diagonal}}{\sigma_{t,max}}$$

$$u_{horiz} = \Delta l_{horiz} = \frac{\Delta l_{diagonal} \cdot b}{l_{diagonal}} \tag{B.3}$$

This gives the spring stiffness for 1 glass plate. The façade is made up of 5 plates. The springs are in parallel configuration; more glass panels result in stiffer behaviour. Note that the wind force is divided over the different glass plates as stated in Equation B.5, and that displacements are the same in each pane as stated in Equation B.6.

$$k_{spring} \ = \ k_{equivalent} \ = \ k_1 \ + \ k_2 \ + \ k_3 \ + \ k_4 \ + \ k_5 \tag{B.4}$$

$$F_{wind} \ = \ F_{eq} \ = \ F_1 \ + \ F_2 \ + \ F_3 \ + \ F_4 \ + \ F_5 \tag{B.5}$$

$$u_{tot} \ = \ u_1 \ = \ u_2 \ = \ u_3 \ = \ u_4 \ = \ u_5 \tag{B.6}$$

When filling in the above formulas for 5 plates with the dimensions 4m x 2m (l x b), the following value for k_{spring} is acquired:

$$k_{\text{spring}} = 158386 \quad \text{N/mm}$$

The way the glass plates are fasten to the roof and floor will influence this value. When soft rubber-like material is used, this stiffness will decrease. This behaviour can be simplified as springs coupled in series. Below is an example of the remaining stiffness when the glass plate is connected with a much less stiff material.

$$k_{\text{eq}} = \frac{1}{\frac{1}{158386} + \frac{1}{10000}} = \ 9406 \quad \text{N/mm}$$

C. Other Diana considerations

C.1 Interface modelling considerations

There are two modelling approaches to simulate the behaviour of the PU interlayer material, which can be seen in Figure C.1. The first approach (Figure C.1a) uses one interface element to model the interlayer behaviour, while the other approach uses 3 components (Figure C.1b).

This second approach accounts for the incompressibility of the interlayer, however it results in considerably longer calculation time as a result of more geometry and finer mesh. The low stiffness properties are assigned to the solid (or other element type) representing the PU, while the interface elements are assigned very stiff properties, stiffer than the surrounding materials. The nonlinear tensile behaviour is still assigned to the interface elements.

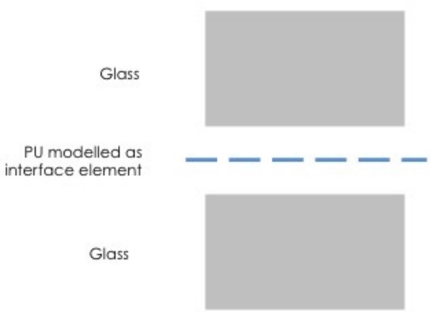

(a)

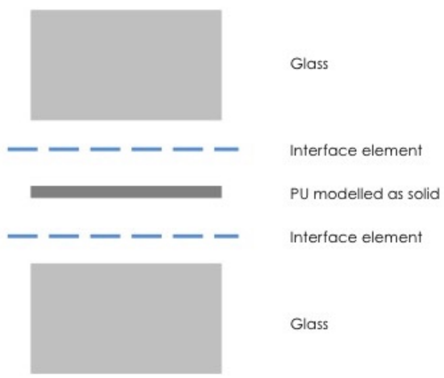

(b)

Figure C.1: The interlayers between the glass components can be modelled in different ways as displayed here, the approach by Aurik (2017) **(a)** and by Jacobs(2017) **(b)**.

Modelling the interlayers as interface elements for this research is based on two considerations. Firstly, there is not enough experimental data available on interlayer behaviour to reliably base the chosen parameters on. Therefore it would still not be certain that the modelled geometry resembles reality accurately. Secondly, investigating the specific parameters for interlayers is outside of the scope of this research. Therefore modelling the interlayers as interface elements is deemed suitable for this research.

D. Loading conditions case study

D.1 Loading conditions

D.1.1 Wind loading

The wind loading has been derived using NEN-EN 1991-1-4.
The most negative situation for the Netherlands a coastal area in wind region I. As reference height for the pavilion z_e = 8m is chosen. This all leads to a peak velocity pressure $q_p(z_e)$: 1,51 kN/m^2.

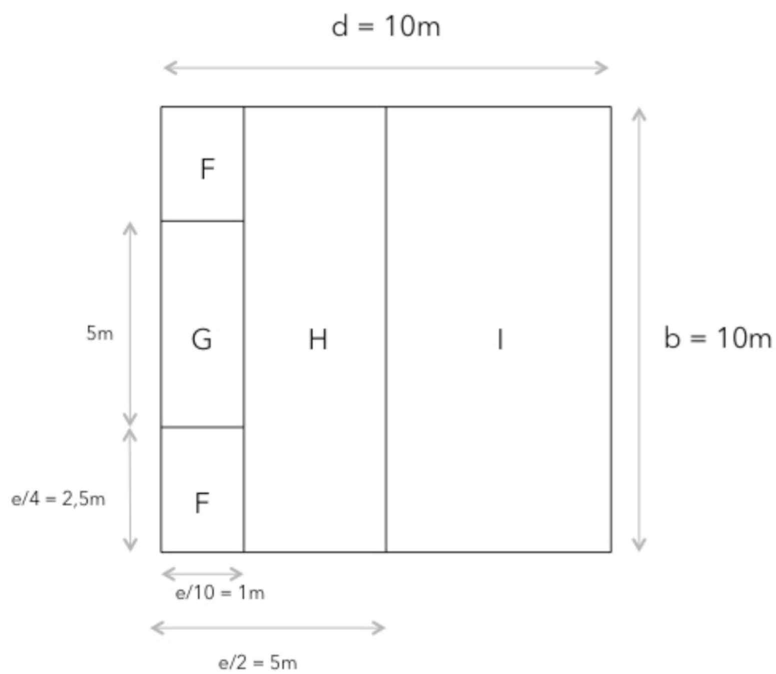

Figure D.1: Wind loading roof according to NEN-EN 1991-1-4

This leads to the following loads for for the roof and façades of the pavilion; half of the pavilion is modelled so the loads act on a depth of 5m.

<u>Wind pressure roof</u>

Wind F	- 2,72	kN/m^2
Wind G	- 1,81	kN/m^2
Wind H	- 1,06	kN/m^2
Wind I	+/- 0,30	kN/m^2

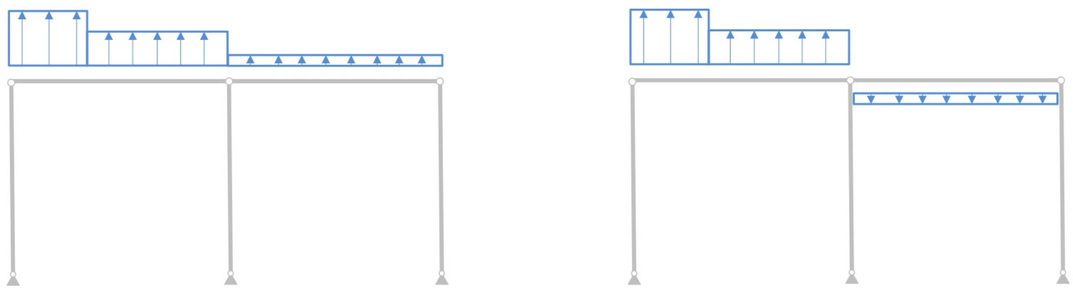

(a) **(b)**

Figure D.2: Wind pressure on the roof with upward Wind I **(a)** and downward Wind I **(b)**.

<u>Wind load facade</u>

Wind D	+ 1,21	kN/m^2
Wind E	- 0,76	kN/m^2

These need to be combined in the most unfavourable way.

D.1.2 Snow loading

For snow loading s = 0,56 kN/m^2 according to NEN-EN 1991-1-3.

D.1.3 Variable roof loading

For category H roofs with roof angle $0 \leq \alpha \leq 15°$ a variable loading of q_k = 1,0 kN/m^2 needs to be accounted for according to NEN-EN 1991-1-1.

D.1.4 Self weight

According to Quick reference a timber roof is 0,36 kN/m^2, which includes timber beams, roof and roof covering. To account for all the timber roof beams it is assumed that the timber roof structure is 0,5 kN/m^2.

The self-weight of all the glass elements is also accounted for: the column, fins and facade: Volume $\times$ 2500 kg/m^3.

D.1.5 Roof ballast

The minimal required roof ballast (if applied) is 0,6 kN/m^2 in order to prevent uplifting of the roof covering. This value is enough to prevent tensile forces in the stacked, glass column. A heavier ballast load of 1,2 kN/m^2 is also investigated in this research.

D.2 Governing loading combinations

This pavilion is considered to be Consequence Class 2 (CC2).

Table D.1: ULS load factors γ

	Permanent loads		**Variable loads**	
Design situation	Unfavourable	Favourable	Leading	Other
I	1,35	0,9	-	1,5
II	1,2	0,9	1,5	1,5

Table D.2: ULS loading combinations

Leading load	**Permanent**	**Wind**	**Snow**	**Variable roof load**
Permanent	1,35	-	-	-
Wind	0,9/1,2	1,5	-	-
Snow	1,2	-	1,5	-
Variable roof load	1,2	-	-	1,5

Note that the factor for combination $\psi_0 = 0$ for snow loading, wind loading and variable roof loading. The combinations therefor only take the leading variable load into account and no accompanying variable loads.

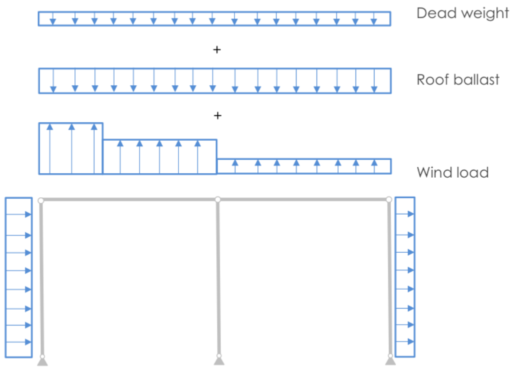

(a)

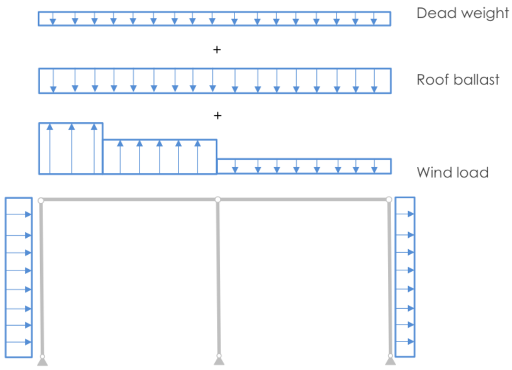

(b)

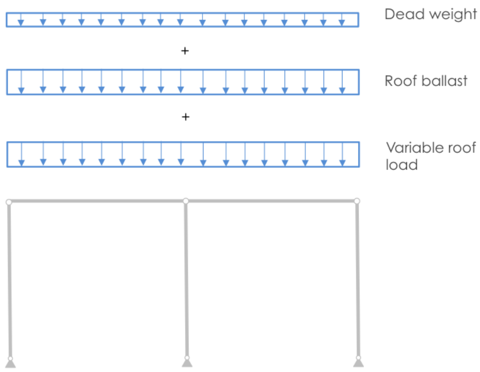

(c)

Figure D.3: Governing loading combinations. LC1 **(a)** LC2 **(b)** and LC3 **(c)**.

E. Load distribution: analytical prediction

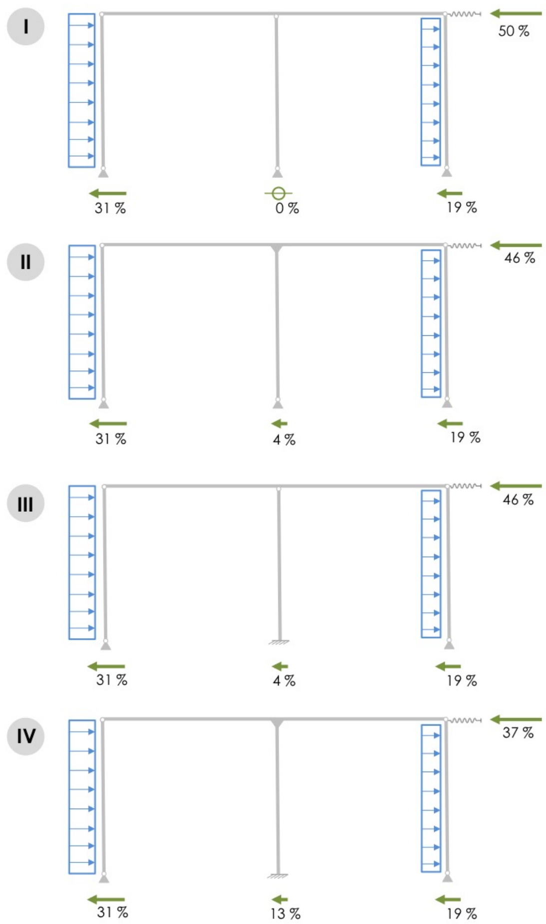

Figure E.1: Schematic image horizontal load distribution following form analytical calculations for different end connections of the central column. The following is kept constand: w=600mm and k_{spring}=8000 N/mm. The distributed load (blue) is horizontal wind load and the green arrows are the reaction forces per element.

Table E.1 shows how different parameters influence the horizontal load distribution within the portal frame. Only with clamped end-connections does the column take up significant amounts of horizontal loading. The remaining 50% of the horizontal load is transferred by the glass façade fins.

Table E.1: Analytical calculations for horizontal load distribution in percentages for different parameter variations

			Horizontal load distribution [%]	
			Glass column	**K_{spring}**
I	w=350 mm	k=8000	0	50
	w=600 mm		0	50
	w=600 mm	k=4000	0	50
II	w=350 mm	k=8000	1	49
	w=600 mm		4	46
	w=600 mm	k=4000	7	43
III	w=350 mm	k=8000	1	49
	w=600 mm		4	46
	w=600 mm	k=4000	8	42
IV	w=350 mm	k=8000	4	46
	w=600 mm		13	37
	w=600 mm	k=4000	20	30

F. Case study design checks

F.1 Design checks glass fins

The maximum allowable horizontal displacement is: $u_{max} \leq \frac{1}{300}h = \frac{1}{300} \times 4000 = 13,3$ mm

The horizontal displacement of the portal depends on the stiffness of k_{spring}; however the structure becomes unstable far below the value of u = 13,33 mm. The value of k_{spring} is set stiff enough to prevent this. The following analytical calculation gives an indication of the required stiffness for k_{spring} in order for the portal to stay within permissible displacements. A portal frame with all hinged connections is unstable. The horizontal load and spring stiffness are linearly related. When limiting the horizontal displacement to the maximum allowable $u_{x,max}$ defined by the Eurocode, derivation of k_{spring} is possible. The horizontal façade load D is governing in this case.

$$k_{spring} \geq \frac{F_{horiz,wind,Dload}}{u_{max}}$$

According to the Eurocode, u_{max} = 13,3 mm, meaning that the minimum value for $k_{spring} \geq 1820$ N/mm. However if u_{max} is required to be smaller, k_{spring} will required to be larger. For example when u_{max} = 2 mm, $k_{spring} \geq 12100$ N/mm.

For the checking maximum allowable displacements we use SLS loading factors. Half way the hinged glass façade fin: $u_{max} = \frac{5}{384}\frac{ql^4}{EI} = \frac{5}{384}\frac{6,05 \cdot 4000^4}{70000 \cdot 9,23e^7}$ = 3,2 mm $\leq$ 13,3mm. So this check for the glass fins is OK.

The tensile stresses stay within the allowable limits for glass.

F.2 Design checks structural façade

As presented in Appendix B, the glass façade is able to take up horizontal wind loading by acting like wind bracings. The cross section of the glass panels ($A_{required}$) is sufficient in order to do so.

F.3 Design checks timber roof

According to NEN 6702 Belastingen en vervormingen TBGB 1990), the maximum allowable roof displacement is:
$w_{max} \leq 0,004 \times l = 0,004 \times 10000\ mm = 40\ mm$

For the displacements, SLS safety factors are used.

The displacements and stresses of the timber roof stay within the allowable limits.

G. Extra drawings pavilion

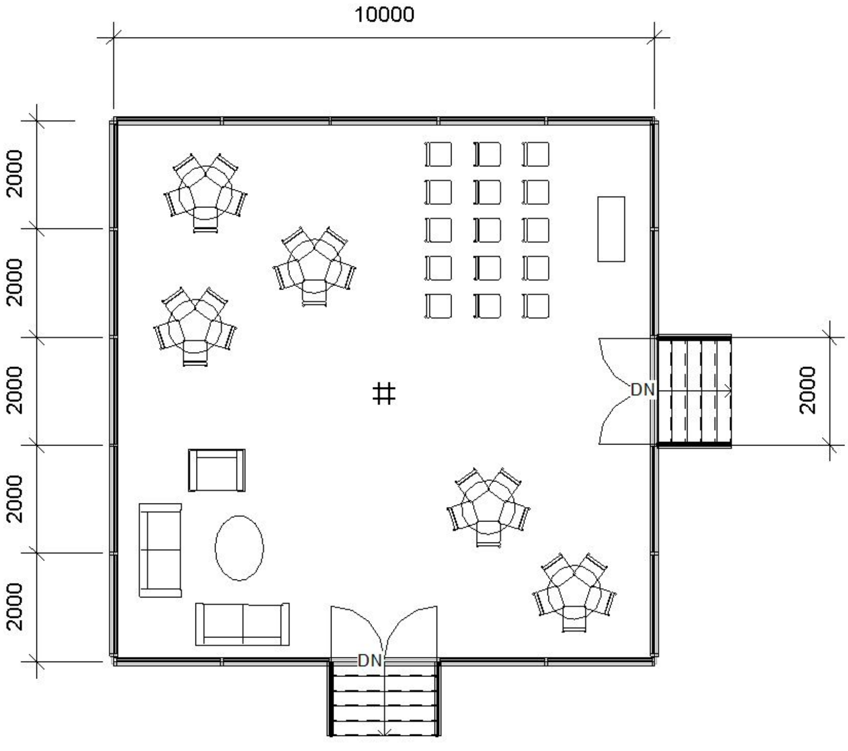

Figure G.1: Floor plan of the pavilion with an example furniture set-up.

Figure G.2: Render of the inside of the pavilion when it is standing on a city square.

Figure G.3: Render of the outside of the pavilion in a park setting.

H. Stress concentrations Diana

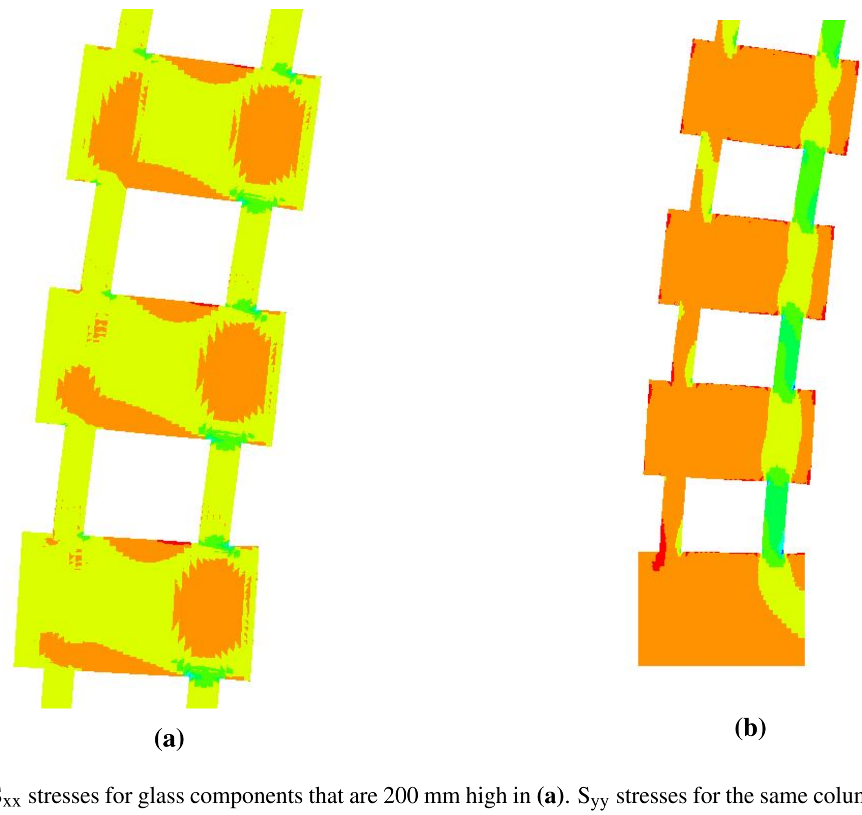

(a) (b)

Figure H.1: S_{xx} stresses for glass components that are 200 mm high in **(a)**. S_{yy} stresses for the same column and loading conditions in **(b)**. The location of the highest tensile stresses can be seen in red.

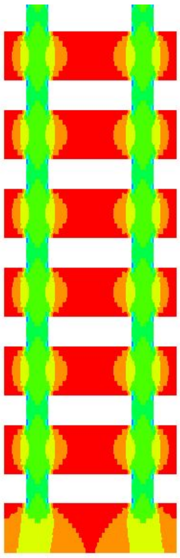

Figure H.2: S_{yy} stresses for loading combination 3